COPPER MINING AND SMELTING TECHNOLOGY IN THE NORTHERN LOWVELD, SOUTH AFRICA, CA. 1000 CE TO CA. 1880 CE

David Killick
School of Anthropology, University of Arizona,
Tucson, AZ 85721-0030, USA
killick@email.arizona.edu

Duncan Miller
Department of Geology, University of the Free State,
Nelson Mandela Drive, Bloemfontein, Brandhof 9324, South Africa

Thomas Panganayi Thondhlana
Department of Archaeology and Museums Studies,
Great Zimbabwe University, Box 1235, Masvingo, Zimbabwe
t.thondhlana@ucl.ac.uk

Marcos Martinón-Torres
UCL Institute of Archaeology
31-34 Gordon Square, WC1H 0PY London (UK)
m.martinon-torres@ucl.ac.uk

ACKNOWLEDGEMENTS

Copper mining and smelting technology in the northern Lowveld, South Africa, ca. 1000 CE to ca. 1880 CE

Killick, D., Miller, D., Thondhlana, T.P. and Martinón-Torres M.

Abstract

We report chemical, petrographic and metallographic studies of copper ores and slags recovered during sporadic surface surveys and excavations over the past fifty years in the Phalaborwa and Murchison Range areas of the northern Lowveld of South Africa. The copper slags around Phalaborwa have unusual mineral assemblages, attributable to the unique geochemistry of the main ore body, the Phalaborwa Complex, where copper minerals were mined from a carbonatite composed of magnetite, calcite and apatite. Strongly reducing conditions had to be avoided to minimise contamination of the copper with iron and phosphorus. As the copper ores contain almost no silicates, silica/alumina flux was added to produce slag. The Precambrian zinc-copper ores of the Murchison Range were also smelted, but during smelting any zinc that was not volatilised was taken up by minerals in the slag, so brass was not produced.

Keywords: Technology; Archaeometallurgy; Copper; Mining; Smelting; Slag; South Africa

1. Introduction

The northern Lowveld (Fig. 1) is in the north-east corner of South Africa, where erosion has exposed the Precambrian basement of the Kaapvaal craton. The Lowveld has a rich archaeological record of settlement during the Late Iron Age (LIA - ca. 1000 cal CE to 1880 CE) linked to exploitation of the salt (Evers, 1974 and Antonites, 2013), iron and copper resources of the region (Miller et al., 2001). A study of iron production in this region during the LIA was recently published by Killick and Miller (2014). The present paper focuses on Late Iron Age copper mining and smelting.

2. Prior studies of metal production in the Lowveld

Comprehensive summaries of historical accounts of metal production and its central economic role in the Lowveld have been published elsewhere (Miller et al., 2001, Miller et al., 2002 and Killick and Miller, 2014). These papers also contain descriptions of the regional and local geology, and of the main archaeological sites from which materials were recovered for analysis. Much of the material discussed here was recovered by N.J. van der Merwe's team in the early 1970s (van der Merwe and Scully, 1971 and Evers and van der Merwe, 1987) and in surveys undertaken by Killick in 1977 and 1978. These collections included ores, furnace slags, primary furnace ingots, cast ingots, and metal artefacts. Killick and Miller worked together on these samples in Tucson in 1998, and also re-examined some

metallurgical specimens previously published in Afrikaans by Verwoerd (1956). Further samples from the collections of the 1970s, and new materials from excavations conducted in 2011 at Phalaborwa, were studied recently by Thondhlana for his doctoral thesis (Thondhlana, 2012 and Thondhlana et al., 2016) under the supervision of Martinón-Torres. This paper focuses on the analysis of copper ores and slags from field surveys and archaeological excavations. Ingots and other copper metal artefacts from Phalaborwa have been described elsewhere (Miller et al., 2001 and Miller, 2010).

3. Geological background to copper mining in the northern Lowveld, ca. 1000 CE – 1880 CE

The major copper deposit in the Lowveld is in the core of the Phalaborwa Complex (Fig. 2 and Fig. 3), a carbonatite volcano (Hanekom et al., 1965, Palabora Mining Company Geological Staff, 1976, Verwoerd, 1986 and Verwoerd and du Toit, 2006) dated radiometrically to 2060 ± 2 Ma (Wu et al., 2011). Before open pit mining commenced in 1965, the surface expression of the central carbonatite pipe was Lolwe Hill (Figs. 3 and 4). The central lobe within the complex is composed of roughly concentric bands of pyroxenite (diopside/phlogopite/apatite rock), phoscorite (olivine/apatite/magnetite rock), and carbonatite (magnesian calcite/magnetite/apatite rock). Copper sulphide minerals (chalcopyrite, valleriite) occur in shear zones in the phoscorite and carbonatite zones. Accessory minerals include phlogopite, chondrodite, baddeleyite, zircon and rare earth oxides (Hanekom et al., 1965 and Palabora Mining Company Geological Staff, 1976).
The precolonial copper mines of Lolwe Hill (no. 4 in Fig. 4) were in the oxidised supergene zone, where copper sulphides had been converted to malachite, azurite and chrysocolla. Preindustrial shafts and galleries on Lolwe Hill were narrow and sinuous to follow rich veins of copper ore (Hanekom et al., 1965, van der Merwe and Scully, 1971 and More, 1974). Lolwe Hill – and almost the entire section shown in Fig. 3 – has since been removed by open-pit-mining, but N.J. van der Merwe was present at the earliest stages of mining in 1965, and was able to obtain specimens of charcoal from prehistoric shafts up to 20 m deep. He obtained three radiocarbon dates from old shafts (Table 1). The oldest (Y-1636; 756–1033 cal CE; 93% probability) predates any currently known Iron Age settlement at Phalaborwa (Evers and van der Merwe, 1987) and may therefore reflect an 'old wood' effect, but Y-1635 (1020–1229 cal CE; 99.1% probability) is contemporary with excavated village sites from which smelted copper has been recovered. Copper was still being mined and smelted here when the German explorer Karl Mauch visited in 1868 (Bernhard, 1971: 41, 54) but had ceased by 1880. Well-preserved copper- and iron-smelting furnaces were still present in the ring of syenite hills around the Phalaborwa carbonatite pipe when open-pit mining began in 1965 (van der Merwe and Scully, 1971 and More, 1974). The descendants of the indigenous metalworkers of Phalaborwa still live in the region, and their oral histories have been collected and analysed – see Miller et al. (2001) for references. Early geological reports also mention 'ancient mines' at the Old Guide Copper Mine and at April Kop (Hall, 1912 and Schwellnus, 1937). The Old Guide Copper Mine (no. 1 in Fig. 4) is located about 7.5 km NNW of the former Lolwe Hill. The deposit is a feldspathic pyroxenite

pipe, presumably connected at depth to the Phalaborwa Complex (Eriksson, 1985). The zone of weathering, with a depth of 6 m, contained copper carbonates (Hall, 1912 and Shand, 1931). 'Ancient workings' were also noted in the deep green pyroxenite east of April Kop, which is 3.5 km south of Lolwe (no. 8 in Fig. 4). Not much is known about this deposit, but the early geological literature indicates that the deeply weathered pyroxenite contained streaks and specks of malachite (Hall, 1912, Shand, 1931 and Schwellnus, 1937). No archaeological excavations have been made at either location.

There is also evidence of pre-European copper mining in the Murchison Range (Fig. 2), a heavily metamorphosed greenstone belt remnant of Precambrian oceanic crust in younger granitic terrain. The Cu-Zn Line of the Murchison Greenstone Belt (Fig. 2) contains 12 small but rich ore deposits of volcanic massive sulphide (VMS) ores.

The 12 VMS ore deposits are spaced at intervals of 7–15 km along the 100 km Cu-Zn Line, but not all are exposed at the present ground surface. The ore deposits contain sphalerite (ZnS), pyrite (FeS) chalcopyrite (CuFeS$_2$) and pyrrhotite (Fe$(1-x)$S), with the proportions of these and several minor minerals varying both spatially and temporally within deposits. Galena (PbS) is seen as massive ore in only one of the deposits. Most of these deposits are much richer in zinc than in copper, but zones of massive chalcopyrite ore have been encountered within several of them (Schwarz-Shampera et al., 2010).

The geological monograph of van Eeden et al. (1939) includes a section on 'ancient workings' in the Murchison Range. We have transferred the locations of these from their map to our Fig. 2. Van Eeden himself noted that:
"All the workings are similar in that they consist of narrow trenches along the strike of the rocks, whereas the European prospecting trenches are across the strike. They are overgrown by bush and trees, some of the latter of considerable age. The conspicuous minerals in the dumps are always malachite and azurite. At the workings east of the United Jack mine pyrite was noticed and in the workings east of Monarch Kop chalcopyrite in a cherty quartzite is in evidence. The writer panned samples from the various workings and found only traces of gold." (van Eeden et al., 1939: 129–130).

All of these 'ancient workings' were on the Cu-Zn Line, except for those east of Monarch Kop. The Monarch Kop workings were in the Antimony Line, which runs parallel to, and to the south of, the Cu-Zn Line (Fig. 2). The high-grade antimony deposits are of almost pure stibnite (Sb$_2$S$_3$) and lack any copper minerals, but the lower grade Complex Antimonial Ores do contain remnant chalcopyrite, although now largely replaced by antimony sulphides (Pearton and Viljoen, 1986). As there is no evidence at all for prehistoric copper-antimony alloys in this region (or anywhere else in sub-Saharan Africa) it appears that the 'ancient working' east of Monarch Kop was on a remnant patch of the original chalcopyrite assemblage, and was therefore mined for copper alone.

One of these 'ancient workings' is the so-called King Solomon's Mine (23° 54.25' S; 30° 38.26' E) on the farm Solomon's Mine 752LT (Fig. 2). When visited by Miller in 1997 the visible precolonial workings consisted of a trench about 120 m long and 4 m wide, but

according to the farmer the trench was much deeper when he was a child, and formerly accessible side adits are now silted up. The only 'ancient workings' in the Murchison Range that have been investigated by geologists are in quartz-chlorite schists just north of the small hills named Kasteelkoppies (Fig. 2), on the farm Vlaglaagte 751LT (van Eeden et al., 1939: 130). Samples from the surface gossan at these workings were examined by the ore microscopist F.C. Partridge, who reported that the primary ore minerals in them were chalcocite and sphalerite, with subordinate chalcopyrite and pyrite, and rare covellite and native copper, in a gangue of iron oxides. He added that '(t)he presence of both copper and zinc minerals in this deposit suggests that the ancients may have obtained a brasslike alloy by smelting the ore' (van Eeden et al., 1939: 141). This speculation has become part of the folklore of the Lowveld (e.g. More, 1974).

The richest ore deposit along the Cu-Zn Line is at the modern Maranda Mine (23° 57.876' S; 30° 27.842' E), located west of the town of Gravelotte (Fig. 2), where the subsurface sulphide ore body contains 17% Zn and 3% Cu. The ore minerals are sphalerite, chalcopyrite, pyrite and pyrrhotite (Viljoen and Reimold, 1999 and Schwarz-Shampera et al., 2010). This lode was not accessible to preindustrial metalworkers, but van Eeden et al. (1939) noted 'ancient workings' in the same stratigraphic horizon roughly nine kilometres east of the Maranda Mine, along the crest of a prominent hill (centre at 23° 56.535' S; 30° 32.249' E) formed by a quartzite layer that dips almost vertically. 'There are numerous trenches along the quartzite and north of the quartzite' (van Eeden et al., 1939: 129). As noted below, the only smelting site recorded so far that can be shown to have smelted zinc-copper ores lies between these trenches and the present Maranda Mine.

In marked contrast to Phalaborwa, there appear to be no oral or written accounts of nineteenth-century mining along the Murchison Range. Nor have any of the copper mines in the Murchison Range been investigated by archaeologists. Evers and van der Berg (1974) did map and partially excavate a prehistoric copper mine at Harmony (24° 11.521' S; 30° 35.622' E), some 25 km south of Gravelotte (Fig. 2). This is in a small greenstone remnant within Archaean granites. The mine consisted of 31 shafts and an open stope over a total length of 400 m, following patchy mineralisation at the schist-granite contact. The low-grade ore contained malachite and azurite. A test excavation revealed a vertical shaft 5.5 m deep leading into a 55° inclined stope. The hanging wall of the stope was still supported by several wooden posts. Rubble fill met the hanging wall at a depth of 14.9 m, so the original depth of the stope could not be determined. The only mining tools found were quartz, quartzite and dolerite hammer stones. Three single-tuyère smelting furnaces were located nearby. A single radiocarbon date (Table 1, RL-207) of 1220–1437 cal CE (2-sigma) was reported on charcoal from a trench dug in centrally situated mine tailings (Evers, 1975 and Evers, 1981). No analyses of ores or slags were reported.

4. Archaeological contexts and chronology

4.1. Sites around the Phalaborwa Complex

The excavated metallurgical remains from Phalaborwa (Miller et al., 2001, Thondhlana, 2012 and Killick and Miller, 2014) came from several clusters of sites on the syenite hills that encircle the Lolwe ore body (no. 4 in Fig. 4).

SHAM1 is a domestic midden associated with extensive evidence of metal production located on the foothill of Shankare (no. 3 in Fig. 4), a prominent syenite hill 4.5 km NE of Lolwe. Initial fieldwork investigations at Shankare during the 1960s by R. Mason revealed at least eight furnaces, an iron forge and terraced platforms (Mason, 1968). J. Pistorius subsequently excavated a copper smelting furnace (SHA2M1), radiocarbon dated (Table 1) to between 1046 and 1277 CE (Pta-4443) (Pistorius, 1989). This date makes Shankare one of three Phalaborwa hills (with Kgopolwe and Nagome) with early second millennium CE occupation and metallurgy (Plug and Pistorius, 1999). The lower slopes to the north of Shankare hill are strewn with large ash middens, rock boulders with dolly holes (depressions produced by crushing ore and/or slag), and scatters of metallurgical debris. Previous investigators concluded that the site was a specialised metal production centre, but efforts during recent fieldwork by Thondhlana to locate further in situ smelting furnaces were unsuccessful. Copper ores, slags and artefacts were recovered from SHAM1, a domestic midden with three radiocarbon determinations (Table 1) between 1022 and 1283 cal CE at 2 sigma. Several other samples studied were recovered during a controlled surface collection exercise from several scatters of metallurgical debris, including crucibles, on the northern foothill of Shankare (Thondhlana, 2012).

On Kgopolwe hill (no. 2 in Fig. 4) N.J. van der Merwe excavated a stratigraphic sequence of three house floors (SPK3) with radiocarbon dates (Y-1637, Y-1639 and Y-1662) between ca. 1040 and 1350 cal CE (Table 1). Specimens SPK3.3 to SPK3.9 and two plano-convex copper ingots, SPK3.A and SPK3.B (Miller, 2010), were found on these floors. Specimen SPK3.10 was probable copper slag found in a whole pot buried beneath overlapping floors of houses 2 and 3 (Evers and van der Merwe, 1987). At the base of the hill, a slag heap (SPK4) with a single date (Y-1657) calibrated to the interval 1290–1470 CE (Table 1) contained both copper and iron slag. Another slag heap (SPK6) is undated and produced both copper- and iron-smelting slag.

A small hill, called Matsepe in some studies (Evers and van der Merwe, 1987, Miller et al., 2001 and Killick and Miller, 2014) and Serotwe in others (Pistorius, 1989 and Thondhlana, 2012), is 4 km west of the former Lolwe Hill ore source (no. 9 in Fig. 4). There were several smelting furnaces and slag heaps at the base of this hill. SPM1 was an intact copper smelting furnace with an oval floor plan, about 0.4 × 0.6 m at floor level, and a domed shaft 0.5 m high with a narrow mouth, and a port or rake hole at floor level for insertion of a single tuyère. Its radiocarbon date (Evers and van der Merwe, 1987) falls in the unhelpfully broad interval 1650–1950 cal CE (Table 1). SPM 2, SPM 3 and SPM 4 are undated slag heaps associated with triangular 3-tuyère iron-smelting furnaces (Pistorius, 1989, Thondhlana, 2012 and Killick and Miller, 2014).

The site MOL1 was a copper smelting site near Molotho hill (no. 7 in Fig. 4), 3.3 km SE of Lolwe, and is now buried under waste from the modern mine. A single-tuyère port furnace (MOL-1) is very similar to SPM1 from Matsepe/Serotwe and also has a radiocarbon date between 1650 and 1950 cal CE (Evers and van der Merwe, 1987: 93; Stuiver and van der Merwe, 1968).

A copper furnace (MN1) at the base of Nagome hill (no. 5 in Fig. 4), 2.5 km E of Lolwe but also now completely buried under waste rock from the modern mine, was very similar to those described above from Matsepe/Serotwe and from Molotho, and also has a radiocarbon date between 1650 and 1950 cal CE (Table 1).

4.2. Sites in the Murchison Range

Our only slag samples that are not from within a 20 km radius of Phalaborwa come from site GM10M (23° 58′ 08″ E; 30° 30′ 40″ S), which lies between the 'ancient workings' on Maranda farm (Fig. 2) and the modern Maranda mine. This is one of twenty five slag heaps documented in the Gravelotte area by van der Merwe's team in 1972–73 (Killick and Miller, 2014, Table 1). In 2001 Miller found another five slag heaps just west of the Maranda Mine. All but GM10M appear to derive from iron smelting. Iron slags from the western Murchison Range contain very high levels of TiO2 (Killick and Miller, 2014) and are black in freshly fractured sections, whereas the GM10M copper slags are light grey. No other copper smelting sites have been reported yet from the Murchison Range, which simply reflects the low intensity of archaeological survey in this area.

5. Analytical methods

The analytical measurements and microscope observations reported here were made at various times over the last forty years. The older bulk chemical analyses of slags were made by wavelength-dispersive X-ray fluorescence (WD-XRF) on glass fusion discs – see Killick and Miller (2014) for details – or by unspecified techniques (Pistorius, 1989). But most of the 'bulk' analyses reported here were made on polished sections in the electron microscope, by averaging energy-dispersive X-ray analysis (SEM-EDS) measurements of several areas of around 2–4 mm2. Most of the optical analysis was done in reflected light (plane- and cross-polarised). Because the bulk chemistries of some of the copper slags are unusual, a few specimens were prepared as polished thin sections for petrographic analysis in transmitted and reflected light, and for electron microprobe analysis of individual minerals.

6. Results

6.1. Presumed copper ores from Shankare and Kgopolwe

Pieces of ore were collected from the same context as other metallurgical debris at Shankare and Kgopolwe. Those from Shankare are from the 2011 excavations (Thondhlana, 2012 and Thondhlana et al., 2016); those from Kgopolwe hill were found in collections from the van der Merwe projects of the 1970s in storage at the University of Cape Town. Two groups of specimens can be distinguished in hand specimen. The first is characterised by oxidised copper minerals with greenish and bluish coloration, non-magnetic and soft, without any visible silicate grains. The second group comprises irregular chunks of magnetite with specks and veinlets of green copper compounds, typical of material from Lolwe.

Sixteen potential ore samples (Table 2) have outer layers of green malachite or bluish azurite, surrounding a red inner matrix of weathered iron and copper oxides, carbonates and/or hydroxides. There are residual inclusions identified as chalcopyrite, chalcocite and barite, enclosed in the weathered iron-copper hydroxide and carbonate matrices. Isolated rare earth oxides and rare earth phosphate inclusions are present in some polished specimens of these slags, indicating their origin in the Phalaborwa Complex.

The 'bulk' composition of these samples (Table 2) show low analytical totals reflecting the inability of SEM-EDS to measure carbon, oxygen and hydrogen in carbonates and hydroxides. The copper oxide

content ranges from about 8 to 60 wt%. Iron oxide (expressed as FeO) in these presumed ores ranges from as little as 0.3 to 63 wt%. Sulphur is low except in one sample (SPK3.1). Although their compositions vary significantly, silica is under 10 wt% in most of these specimens, and alumina is essentially absent. These results reflect the unusual geology of the carbonatite pipe, in which silicates and aluminosilicates are very minor components (Palabora Mining Company Geological Staff, 1976).

6.2. Slags from the Shankare midden deposits

The charcoal impressions in Shankare slags show that these solidified inside furnaces. Most are very small, with an average mass of only 15 g. The majority probably were deliberately crushed after smelting to release embedded copper prills, as recorded elsewhere in South Africa (e.g. Hall et al., 2006). The sectioned copper slags contain visible copper prills together with partially reduced and unreacted mineral inclusions in their matrix. The unreacted mineral inclusions were identified as magnetite, apatite (e.g. Fig 5), quartz and chalcopyrite. The residual magnetite grains in these copper slags contain magnesia and alumina up to 3 and 4 wt% respectively, without any detectable TiO2.

Twenty seven copper smelting slag samples from different contexts at Shankare were subjected to detailed microscopy and chemical investigations (Table 3). The principal oxides in these SEM-EDS analyses are SiO_2 (29–51 wt%), FeO (6–45 wt%), CaO (8–28 wt%) and P_2O_5 (1–12 wt%). Two bulk analyses of powdered samples of Shankare slag were published by Pistorius (1989: Table 17) and are reproduced here in Table 4. These have higher silica, and lower iron and calcium oxide, possibly reflecting undissolved silica inclusions in these whole-sample analyses. (The areas analysed by SEM-EDS were chosen to avoid undissolved inclusions such as those in Fig. 5.) The high silica contents in both sets of slag analyses are noteworthy, given that there is so little silica in the ore samples.

The Shankare slags have heterogeneous microstructures, with undissolved magnetite, apatite and quartz in a crystalline matrix dominated by blocky olivines, magnetite spinels, copper prills and a small proportion of interstitial glass. The olivines are fayalitic with a one third forsterite component. These blocky olivines together with residual minerals, like apatite and in one instance chalcopyrite, justify the identification of these slags as smelting debris rather than refining debris (Thondhlana, 2012). A significant level of P_2O_5 (up to 12 wt%) is present in the matrix of some Shankare slags.

The slags from Shankare contain entrapped spherical copper prills, with diameters ranging from a few microns up to 2 mm. The prills usually have significant impurities in the form of sulphides and metallic iron (Fig. 6), but no tin or zinc were detected by SEM-EDS. Some of the larger copper prills (>1 mm) contain up to 30 wt% Fe. Both copper sulphide and copper-iron sulphide inclusions were noted in copper prills. These certainly derive from residual sulphides in the ore.

6.3. Slags from the Molotho furnace

Six slag specimens from the single-tuyère furnace at Molotho were prepared by Thondhlana as polished blocks. The samples weighed between 12 g and 33 g and were strongly magnetic. Their exterior surfaces had many charcoal impressions without any visible unreacted minerals. The 'bulk' chemical analyses of the Molotho slags (Table 3) show that the principal oxides are SiO_2 (33–46 wt%), CaO (23–27 wt%) and FeO (18–31 wt%) (Thondhlana, 2012). These slags have relatively low levels of iron oxide, surpassed by both silica and lime. Apart from these three principal oxides, these slags have significant levels of MgO (2–12 wt%). The low P2O5 levels (0.7–1.2 wt%) in the Molotho copper slags contrast strongly with the high levels of P2O5 documented in the Shankare slags, indicating either the use of a different source of ore, or beneficiation of ores by the Molotho smelters to exclude apatite.

Microscopically, the Molotho slag samples are homogeneous, dominated mostly by blocky silicates and magnetite spinels together with tiny copper prills. Their microstructure contrasts with the heterogeneous nature of copper smelting slags from Shankare described above. Occasional wüstite (FeO) globules are present in the copper slags from Molotho. Abundant, rounded copper prills rarely exceeding 10 μm in diameter are relatively pure, with few globular light blue inclusions identified as chalcocite. None of these slag-entrapped copper prills show microscopic evidence of exsolved iron, nor any other base metals, suggesting that only unalloyed copper was produced.

SEM-EDS analyses of selected silicate crystals in Molotho slags are provided in Table 5 (converted from the atomic percent values in Thondhlana (2012: Table 7.7)). All of the analyses show very high CaO, and highly variable FeO, MgO and SiO_2. Identification of these crystals was enabled by petrographic and electron microprobe analysis of a polished thin section from Molotho. This contains four separate flows welded together, varying greatly in chemical composition and texture. At one end of this range of variation are portions that are mostly opaque. The opaque phases are copper metal with magnetite in some areas, and copper with metallic iron in others. At the other end of the range of variation are flows that consist mostly of large transparent crystals (Fig. 7). In transmitted light two types of crystals were noted: (1) melilites with low birefringence (often anomalous), as rectangular laths sometimes showing characteristic 'peg structure' perpendicular to their lengths, and (2) crystals with high first/low second order birefringence and straight extinction.

Electron microprobe analyses (Table 6, analyses 1 through 15) identify the melilites as fairly consistent solid solutions of ferroåkermanite ($Ca_2Fe_2+Si_2O_7$) in åkermanite ($Ca_2MgSi_2O_7$). The second silicate (Table 6: analyses 16 through 27) is an orthosilicate in the continuous solid-solution series between monticellite ($CaMgSiO_4$) and kirschsteinite ($CaFeSiO_4$). The cores are roughly 50% monticellite, 50% kirschsteinite, but the rims are much richer in the kirschsteinite molecule. The opaque minerals (Table 6, analyses 28 through 35) are magnetite with very low TiO_2.

6.4. Slags from the Kgopolwe smelting and habitation sites

The whole pot excavated from beneath the floors of Houses 2 and 3, Unit 7 at SPK3 on Kgopolwe (Evers and van der Merwe, 1987) contained 256.5 g of slag nodules as well as two human finger bones. One slag nodule (mass 38.5 g) was homogenised by grinding to a powder and analysed by WD-XRF (Table 4, analysis SPK3.10). It is a silicate slag rich in iron, low in calcium, and containing about 0.1 wt% copper. Another slag nodule (SPK3.10a) with a mass of 78.0 g was thin sectioned and examined by SEM-EDS. The 'bulk' composition (Table 3, analyses SPK 3.10a and SPK 3.10b) is similar to that of the WD-XRF analysis of the previous nodule. The microstructure shows both wüstite (Table 5, analysis 10) and magnetite dendrites, though not together in the same fields of view. Laths of fayalite (Table 5, analysis 9) and interstitial glass (Table 5, analyses 7 and 8) are present throughout. There are sporadic crystals of leucite, areas with cotectic intergrowths of leucite and wüstite, and sparse glassy areas containing bireflective plates of delafossite. Numerous rounded droplets of copper and iron are present. Metallic iron and delafossite are thermodynamically incompatible (Hauptmann, 2007) so their occurrence in the same sample must mean that there was great variation in the partial pressure of oxygen during this smelting operation. With so little copper present, it is difficult to say with certainty whether these slags were the product of copper smelting or iron smelting furnaces.

Three porous, weakly magnetic slag nodules were found in excavation unit 12 of SPK3. The largest (SPK 3.13) was sectioned and polished for metallography and analysis by SEM-EDS. The 'bulk' analysis (Table 3, analysis SPK 3.13) is very different from those of SPK 3.10, with 25 wt% each of CaO and FeO. The microstructure shows masses of cuprite, metallic copper droplets containing a few

percent iron, delafossite, magnetite and minute laths of a magnesium-calcium-iron silicate phase, possibly a melilite (Table 5, analysis 12). Alumina, the alkalis and phosphorus are concentrated in the residual glass (Table 5, analyses 11 and 13).

Two polished blocks and one thin section of slag from SPK4 were studied. One block is very porous, due to gas trapped during solidification. It consists of angular crystals of titaniferous magnetite and blocky fayalite laths (identified by SEM), in a groundmass of smaller fayalite laths, numerous small rounded copper droplets, and highly bireflectant needles of delafossite. The other block and the thin section are relatively iron-poor and dominated by felted silicate laths with copper drops but almost no spinels. In the thin section the first phase to crystallise is identifiable in thin sections as a clinopyroxene (phase 1 in Fig. 8). This was followed by apparently simultaneous crystallisation of zoned anhedral crystals of olivine (phase 2) and anhedral calcium phosphate (phase 3). Between these is a small amount of glass containing tiny magnetite rhombs in glass. Electron microprobe analyses of the silicates are shown in Table 7. When recalculated as percentages of the $Ca_2Si_2O_6$, $Mg_2Si_2O_6$ and $Fe_2Si_2O_6$ molecules and plotted on the diagram of Morimoto et al. (1988) these pyroxenes fall in the field for diopside (Fig. 9). The cores of the olivines (Table 7, analyses 13, 14, 15, 17, 18, 20, 21,) are intermediate between forsterite and fayalite, but become increasingly fayalitic towards the rims (Table 7, analyses 16, 19, 22). A very unusual feature of the olivine analyses is the presence of between 0.2 and 1.6 wt% P_2O_5 – phosphorus presumably substitutes for silica in the olivine lattice. Cloudy areas in the thin section, enclosing many small bubbles and tiny birefringent crystals, appear to be carbonates that had lost CO_2 and were in the process of forming silicate minerals.

A polished block and a thin section from the SPK6 slag heap contain large copper drops, with inclusions of sulphide and metallic iron (often enclosed in sulphide envelopes) in a slag of silicates, spinels and glass. In the polished thin section the undigested magnetite grains are up to 4 mm in size and may contain small crystals of apatite. The larger silicate phenocrysts are olivines. In between these are tiny late-forming crystals of a green mineral in a brown glass. These crystals are too small to identify, but appear to be the same mineral that is positively identified as hedenbergite in slags at Matsepe/Serotwe (see below).

6.5. Copper smelting slags from Matsepe/Serotwe

Table 4, analysis SPM1a is a WD-XRF analysis on glass fusion discs of a bulk sample of slag from van der Merwe's 1972 excavations. This analysis has much higher TiO_2 content than any other copper slag discussed here. The concentration of TiO_2 in magnetite within the Phalaborwa Complex shows strong zoning (Palabora Mining Company Geological Staff, 1976: Fig. 10). Magnetite from the central Transgressive Carbonatite (Fig. 3), in which the Lolwe copper mines were located, has TiO_2 below 0.1 wt%. Magnetite in the Banded Carbonatite has up to 1 wt%, those from the phoscorite up to 3 wt%, and those in the pyroxenite 4–8 wt%. Analysed prehistoric iron smelting slags around Phalaborwa almost all contain 4–8 wt% TiO_2 (Killick, 1977, Thondhlana, 2012 and Killick and Miller, 2014), while all copper smelting slags except for this sample have less than 1 wt% TiO_2 (Table 3 and Table 4). As previously noted, there were two precolonial copper mines in the pyroxenite – at the Old Guide Mine and at April Kop (Fig. 4). It therefore seems likely that this slag sample derives from smelting of ore from one of these mines. April Kop (no. 8 in Fig. 4) is the closer of the two to Matsepe/Serotwe (no. 9 in Fig. 4).

SEM-EDS 'bulk' analyses for four single pieces of slag from SPM-1 (Thondhlana, 2012: Table 7.11, and this paper, Table 3) give consistent compositions that are very different from that of the WD-XRF sample. These closely resemble the analyses of other copper slags (Table 3 and Table 4) in their high

CaO content (15–20 wt%) and low TiO2 (0.2–0.3 wt%). Clearly these derive from ores from the Transgressive Carbonatite.

In reflected light seven polished blocks show numerous tiny sub-spherical copper droplets (many in envelopes of copper-iron sulphides), relatively few skeletal rhombs of magnetite and elongated laths of two silicate minerals of different reflectivities. One specimen has numerous small bireflectant plates of delafossite.

In two thin sections the mineral assemblage is somewhat different. In reflected light copper drops, some with envelopes of sulphides, and rhombs of magnetite are common. In transmitted light melilite crystals are present but are much less common than those of a different silicate, which is pleochroic from very pale pink to very pale blue in PPL (Fig. 10a), and occurs as euhedral rhombs and stubby subhedral laths without obvious cleavages. While the latter mineral looks like an olivine in PPL, its maximum birefringence in XPL is in the mid-second order, too low for fayalite or kirchsteinite (Fig. 10b). These crystals often have rims of higher birefringence than the cores. These two colourless silicates are accompanied by a third silicate, pleochroic from grass-green to orange-brown (Fig. 10a). This appears to be the same mineral noted in the covered thin section from SPM1 and in the thin section from SPK4.

Electron microprobe analyses of these silicate crystals are given in Table 8 and Table 9. One of these crystals (Table 8, analysis 1) is a melilite with a composition between åkermanite and iron åkermanite. Analyses 2 through 28 are on the pale pink/pale blue silicates described above and correspond to what Deer et al. (1997: 372) call ferroan monticellites. These fall along the solid solution series from monticellite to kirschsteinite. Analyses 9 and 11 are of rims on the crystals whose core compositions are analyses 8 and 10 respectively. Both rims have much lower MgO and much higher FeO than the cores of their respective crystals, and are therefore magnesian kirschsteinite. The final phase to crystallise in this slag is the mineral showing green to orange-brown pleochroism. Electron microprobe analyses of this mineral are shown in Table 10, and as analyses recalculated (1) to include ferric iron for charge balance in the pyroxene structure and (2) as percentages of hypothetical pyroxene end members. When these end member percentages are transferred to the triangular diagram for Ca-Mg-Fe pyroxene compositions (Fig. 9), all fall in the field for hedenbergite.

Compositions of 16 spinels in this thin section were also obtained by electron microprobe. TiO_2 contents are consistently under 0.5 wt%, Al_2O_3 around 1.5 wt% and MgO between 1.4 and 2.0 wt%. Cr_2O_3 and V_2O_5 are always below the limits of detection.

With secure identifications of these phases provided by petrography and electron microprobe, we could return to the SEM-EDS analyses of crystals in Table 5 (analyses 14 through 17) and tentatively identify most of the mineral phases that these analyses represent.

6.6. Other copper smelting sites at Phalaborwa

Bulk analyses for copper smelting slags from other sites within a 15 km radius of the former Lolwe Hill are given in Table 4. Analyses SPM1a and SPK3.10 have already been discussed. The other analyses were made by FOSKOR (the corporation that mines phosphate at Phalaborwa) (Pistorius, 1989). The techniques used to obtain these analyses were not specified, and some analyses are obviously incomplete (lacking TiO_2, P_2O_5 and volatiles), but the values for other major elements are in reasonably good agreement with those obtained by SEM-EDS on the Shankare, Molotho and Matsepe/Serotwe copper slags discussed above. Note in particular the very high CaO for most slags. SiO_2 is generally higher in the WD-XRF

bulk analyses (Table 4) than in the SEM-EDS 'bulk' analyses (Table 3). This is probably because the areas chosen for analysis by SEM-EDS deliberately avoided unreacted mineral inclusions, some of which are of quartz, but these are included in WD-XRF analyses, which are of powdered slags.

6.7. Slags from Maranda smelting site GM10M

Although there is substantial evidence of precolonial mining in the Murchison Range (Fig. 2), GM10M is the only copper smelting site yet found in this area. It is located west of Gravelotte (Fig. 1 and Fig. 2) on the farm Maranda 675LT (23° 58' 08" S; 30° 30' 40" E). This slag heap was noticeably different from the many heaps of iron smelting slag along the Murchison Range because of its colour – medium grey on a freshly fractured surface, whereas the iron slags in this western Murchison area are black (Killick and Miller, 2014).

Thondhlana (2012) examined one piece of copper slag from this site. It had a mass of 17 g, was weakly magnetic, and had a smooth surface without any external porosity, suggesting that it was once highly fluid. A polished block shows small elongated skeletal silicate crystals, indicating rapid cooling, and subcubic magnetite spinels, abundant light blue sulphide matte prills and smaller metallic copper prills. Area analyses of several matte prills with SEM-EDS revealed sulphur levels of up to 23 wt%, with iron of up to 1 wt% and the balance copper – a composition that approximates chalcocite. Table 10 shows the average 'bulk' analysis of this specimen by SEM-EDS. The major points of interest here are (1) that CaO (3.0 wt%) and MgO (0.5 wt%) are very low in comparison to most Phalaborwa copper slags, and (2) the presence of 1.2 wt% ZnO. The copper prills do not contain detectable zinc.

In reflected light a polished thin section of a second piece of slag also shows tiny silicate laths, small subcubic spinels, and subspherical prills of sulphides and copper. There are no unreacted ore minerals or quartz. The silicate crystals were too small for optical identification, but electron microprobe analysis shows that at least three different silicate minerals are present (Table 10). These are fayalite and two minerals, tentatively identified as pyroxenes, that would plot near the wollastonite-ferrosilite edge of the pyroxene compositional triangle in Fig. 9. All three silicates and the spinel (magnetite) contain appreciable ZnO.

Only 15 of 54 copper prills analysed by electron microprobe in three polished blocks of slags from GM10M contain zinc above the limit of detection (average 0.05 wt% Zn) and only five have more than 0.3 wt% Zn. Thus most of the zinc in the ore must have boiled off (the boiling point of metallic zinc is 907 °C), with only a small amount passing into the slag. There is a substantial amount of metallic iron in some copper prills – there is even one iron prill with 5 wt% Cu. Metallic iron is thermodynamically incompatible with the inferred presence of ferric iron in magnetite and in the pyroxenes, indicating that there was a substantial increase in the partial pressure of oxygen (pO_2) as the slag was starting to crystallise. In terms of process, this may mean that the bellows were withdrawn from the tuyères while the slag was still liquid.

7. Discussion

7.1. Ores and furnace design

The ore samples recovered from Shankare and Kgopolwe are largely carbonates (malachite and azurite), often enclosing, or intergrown with, magnetite and apatite crystals. Tiny crystals of rare earth oxides in these ores reflect the concentration of these elements in the carbonatite magma (Verwoerd, 1986). Chalcopyrite was noted as a minor phase in the copper carbonate ore samples

from Shankare and Molotho, but there is no evidence for smelting of the primary sulphide ore at Phalaborwa, or anywhere else in southern Africa. The sulphide inclusions commonly seen in southern African smelted copper derive from minor residual sulphides in the oxide and carbonate ores (Miller, 2010).

Archaeological evidence shows that at least two types of smelting furnace were employed in the northern Lowveld after 1000 cal CE. Forced-draft shaft furnaces 1.0–1.2 m tall with three tuyères (presumably blown by leather bag bellows) and either triangular or cylindrical plans were used to smelt iron (Evers and van der Merwe, 1987 and van der Merwe and Killick, 1979). A much smaller domed furnace, about 50 cm in internal diameter, 30–40 cm high, blown through a single tuyère, served for smelting copper (illustrated in More, 1974; in Miller et al., 2001). Finds of both copper smelting and iron smelting slags in some slag heaps adjacent to examples of the larger furnaces (as at SPK6) may perhaps indicate that sometimes copper was smelted in the larger type of furnace.

The copper workers had to avoid creating too reducing a furnace atmosphere, which would contaminate the copper with metallic iron. Even in the smaller furnaces, the atmosphere sometimes became over-reducing, as is shown by free iron droplets and the iron in the copper prills trapped in some of the slags. The smaller furnaces did not form pools of liquid slag, so the copper slags solidified among charcoal and are highly variable in chemistry and in mineral assemblages.

The chemistry of the carbonatite ore body posed complex problems for the copper workers. There is very little silica in the carbonatite, so silica had to be added to the furnace charge to remove the iron, magnesium and calcium oxides as liquid slag. Some silica in the slags may have come from reaction with the clay tuyères or furnace wall, but the ratios of silica to alumina in the slags (Table 3 and Table 4) are mostly much greater than the 2:1 to 4:1 ratios in clay minerals, so the slags cannot have been formed entirely, or even predominantly, by reaction between ore and furnace ceramic. We have shown elsewhere that silica flux – probably quartz sand from the erosion of the Archaean granites – was added with the magnetite ore when smelting iron at Phalaborwa (Killick and Miller, 2014). It is quite clear from our analyses that silica was also added when smelting the silica-poor copper ores from the Phalaborwa carbonatite, as undigested grains of quartz are often seen in the slags.

Phalaborwa copper workers faced another unusual problem, in that the copper oxide minerals are associated with apatite. When lack of care in the choice of ore was combined with an over-reducing furnace, the copper could be contaminated with iron phosphide. The bimetallic Verwoerd A ingot found near Lolwe (Verwoerd, 1956 and Miller, 2010) is proof that sometimes this mistake was made. This is a surface find that has a layer of copper, contaminated with metallic iron and copper-iron sulphides, under a layer of a brittle iron-phosphorus alloy containing copper dendrites. Undigested apatite was present in the Shankare slags, which date to the early second millennium CE, and calcium phosphate was precipitated from the molten slag at SPK4, which is undated (Fig. 8). But copper slags from the later dated contexts like Molotho and Matsepe had lower P_2O_5, and no undigested apatite or crystallised calcium phosphate was noted in these. This implies that the later smelters hand-sorted ores to remove pieces with visible apatite. Although the apatite in the ore-body is blue-green in colour, its vitreous lustre and crystalline morphology make it relatively easy to distinguish from the earthy and amorphous blue and green copper carbonates.

7.2. Copper slags
Two chemical tendencies can be seen in the copper-smelting slags – the relatively iron-rich and the relatively iron-poor slags. The iron-rich copper-bearing slags had primary rhombs or dendrites of magnetite with fayalitic olivine as the dominant silicate. These typically had less than 10 wt% CaO +

MgO and more than 50 wt% FeO + Fe_2O_3 (Table 3 and Table 4). Most of the slags of this tendency in our sample are from the sites at Kgopolwe Hill (labels starting with SPK). Some of these have more than 1 wt% TiO_2 (Table 3 and Table 4) and thus may derive from ores from the Old Guide Mine pyroxenite, which is closer to Kgopolwe than is the Lolwe ore body (Fig. 4).

The iron-poor copper slags had varying combinations of pyroxenes (diopside-hedenbergite series), melilites (åkermanite-ferroåkermanite series) and orthosilicates (monticellite-kirschsteinite series), with only small amounts of magnetite. They typically contained at least 20 wt% CaO + MgO, and less than 35 wt% FeO + Fe_2O_3 (Table 3 and Table 4). It is worth noting that anorthite ($CaAl_2Si_3O_8$), which is often noted in calcareous copper smelting slags, is absent from our samples, probably because the concentration of alumina is unusually low. The high MgO and very low TiO_2 contents in the iron-poor slags clearly imply that the parent ores for their slags came from the Transgressive Carbonatite (Fig. 3), which once formed Lolwe Hill.

This variation in chemical and mineralogical composition reflects variation in the combination of minerals in individual lumps of ore. On occasion a single thin section (like that described above from SPK4) may have flows with both of these chemical tendencies. This extreme heterogeneity accounts for the lack of fit that we sometimes observed between WD-XRF bulk chemical analyses – samples from powders made from large samples of slag (100–500 g) – and the mineral composition observed in individual thin sections or polished blocks. The remarkable variation noted in this slag is a consequence of the process employed to smelt them. Slag was not tapped from these furnaces, and does not appear to have formed pools of liquid slag – most of the slags clearly solidified around pieces of charcoal.

The two plano-convex primary copper ingots SPK3A and SPK3B from Kgopolwe, dated to the eleventh or twelfth centuries, have charcoal-embedded slag adhering to their bases (Miller et al., 2001 and Miller, 2010) and thus clearly solidified within furnaces. Since the later copper smelting furnaces are of the same design as the earlier ones, we assume that tapping of liquid copper was not practised at any point. We infer that most of the copper separated cleanly from the slag because we see no evidence for crushing of slag. This in turn implies that the operating temperatures of the small domed furnaces were well above the melting point of copper (1084.6 °C), but not far enough above the melting points of the slags to allow the latter to drain freely to the base of the furnace. The compositions of the slags are too complex to justify combining elements to fit simplified compositions to the usual ternary and pseudoternary equilibrium diagrams applied to slags, so we are not able to estimate the free-running temperatures.

These Phalaborwa copper slags are unlike any copper slags yet noted in Africa, but do have some mineralogical similarities to certain Bronze Age slags from Feynan in Jordan, dated to the fourth millennium cal BCE (Hauptmann, 2007). At Feynan slags were produced by smelting the sedimentary ores of the DHS horizon, which are low in iron but rich in calcium, magnesium and phosphorus. Like the Phalaborwa slags, these slags contain melilites, and also clinopyroxenes in the diopside-hedenbergite series. Some Feynan copper metal even contains inclusions of iron phosphide. However, the Feynan DHS ores did contain enough silica to produce slags without the addition of silica flux. In this respect the technology used at Feynan was very different from that developed at Phalaborwa.

7.3. Iron and phosphorus in copper

The high level of phosphorus (as apatite) and iron (as magnetite) in Phalaborwa copper ores could cause problems if the furnace atmosphere was too reducing, as is illustrated by the bimetallic Verwoerd A specimen (Miller, 2010). It was perhaps because of this problem that different furnaces

were developed for iron smelting and copper smelting. The earliest known example of the small domed copper smelting furnace with one tuyère is from Shankare, dated between the mid-eleventh and mid thirteenth centuries cal CE (Table 1).

Copper prills in some of the slags are contaminated with metallic iron, showing that the Phalaborwa smelters often had difficulty in controlling the reducing furnace atmosphere. In this connection we note an account, given in 1940 by M.F. Mamadi to the ethnographer N.J. van Warmelo, of the oral traditions of the Musina clan, who worked the major copper deposit at Messina in the western Soutpansberg, some 250 km north west of Phalaborwa (van Warmelo, 1940). These traditions claim that before settling at Messina the Musina clan had exploited the Phalaborwa ore body, but had abandoned it because copper contamination had 'weakened' the iron. The name given to the copper contamination was musina, meaning 'that which spoils' (van Warmelo, 1940 and Hanisch, 1974). While the Verwoerd A ingot provides a dramatic illustration of this problem, we choose to interpret this account more broadly as the recognition by indigenous metalworkers of the polymetallic nature of the ore body, and of problems encountered in the separation of the metals.

Iron contamination in copper could be removed through a refining process of melting the copper in crucibles, such as those found at Shankare (Thondhlana, 2012). Small iron droplets would float to the top of the molten copper and would be oxidised to dross that could be skimmed off (Thondhlana et al., 2016). This process has been recorded in some detail at the nineteenth century site of Marothodi near Rustenburg (Hall et al., 2006). Concentrations of iron in the analyses of copper artefacts recovered from Phalaborwa sites are all below 0.5 wt% (Killick & Miller, in preparation).

7.4. Trends in smelting technology through time

There appears to have been a hiatus in human occupation at Phalaborwa between the fifteenth and seventeenth centuries CE (see plot of calibrated radiocarbon dates in Miller et al., 2001: Fig. 2). If we treat slag assemblages from Shankare and Kgopolwe as representative of earlier material, and those from Matsepe and Molotho as representative of the later sites, then we tentatively can identify technological changes through time. Copper smelting slags from Shankare and Kgopolwe contain more residual minerals, higher levels of iron oxide and phosphate, and copper prills with exsolved iron. The absence of residual minerals and copper prills with exsolved iron in the Matsepe and Molotho slags points to refinement of extraction methods, such as balance in redox and temperature together with use of well beneficiated ores. The high phosphate levels in Shankare slags entered the smelting system from the gangue apatite as discussed above, while high iron oxide levels together with co-smelting of copper and iron shows unbalanced redox and temperature regimes. Neither of these problems is evident in the later materials from Matsepe and Molotho.

7.5. Zinc and brass

The geologist F.C. Partridge (in van Eeden et al., 1939: 141) was the first to suggest that prehistoric smelting of the zinc-copper ores of the Murchison Range may have produced brass (see also More, 1974: 230). This claim was repeated to van der Merwe and Killick during fieldwork in the 1970s by several geologists at Lowveld mines, but seems highly unlikely on thermodynamic grounds. Zinc metal boils at 907 °C, so any zinc oxide that was reduced to metal should be rapidly lost as vapour from a smelting furnace. Any unreduced ZnO should pass into the slag. This is exactly what we have found in examination of slag from GM10M, the only smelting site yet found that used the Zn-Cu ores of the Murchison Range. It should lay to rest the myth of 'natural brass' production in the Lowveld.

8. Conclusions

We have presented a compendium of archaeological and archaeometric data from field research carried out over the last fifty years, relating to copper production in the northern half of the South African Lowveld. Although copper artefacts occur in archaeological sites in other parts of Southern Africa from around 300 cal CE, the available radiocarbon dates suggest that the Phalaborwa ore body was not exploited until about 1000 cal CE. Thereafter both copper and iron were smelted at Phalaborwa. Copper carbonate ores were mined from shallow shafts and adits (up to 20 m deep) but iron ore was not mined, as vast quantities of magnetite were available as surface scree (Killick and Miller, 2014).

Copper oxide minerals were obtained from a very unusual ore body (a carbonatite) composed of magnesian calcite, magnetite and apatite, but almost devoid of silicates. To smelt these ores, copper workers had to invert their usual practice, which was to use iron oxide flux to remove silica and alumina gangue as a molten slag. At Phalaborwa the copper workers had to add quartz sand with the ore to remove calcium, iron, magnesium and phosphorus as a molten slag. Iron workers at Phalaborwa (and elsewhere in the Lowveld) did likewise, adding silica to make slag when smelting magnetite and magnetite-ilmenite ores, which contain almost no silica (Killick and Miller, 2014). We suggest that the need to develop these new smelting techniques may account in part for the lack of evidence for extractive metallurgy at Phalaborwa before about 1000 cal CE.

8.1. Priorities for future research

The scale of copper smelting at Phalaborwa cannot yet be estimated. There are remains of copper smelting around at least twelve of the syenite hills that form the outer ring of the Phalaborwa Complex (Evers and van der Merwe, 1987 and Pistorius, 1989) but no attempt has been made to estimate the volume of copper slag on each of them. Future attempts to make such estimates will be complicated by the fact that our work shows that some heaps contain both copper slags and iron slags, and by the burial of some of these hills under modern mining dumps (Fig. 4).

We do not yet have any evidence for how far Phalaborwa copper was distributed. The most promising technique for documenting this is lead isotope ratio analysis, which has only just begun to be applied in southern Africa (Molofsky et al., 2014). Copper was smelted in many other parts of southern Africa before the arrival of European colonists (van Warmelo, 1940, Hanisch, 1974, Huffman et al., 1995, Hall et al., 2006, Miller, 2002, Grant and Huffman, 2007, Miller and Hall, 2008 and Miller, 2010), so the first task in tracking archaeological copper ingots and artefacts to their geological sources will be to determine whether these ore sources can be distinguished by their lead isotope ratios.

Although there is abundant evidence for pre-European copper mining in the Murchison Greenstone Belt, none of these mines have been studied by archaeologists. Only one copper-smelting site (GM10M) has been recorded along the Murchison Range, so we assume that many more await discovery. Archaeometallurgical studies should also be made of the ores and slags excavated at the Harmony mining/smelting complex (Fig. 1; Evers and van der Berg, 1974).

References

Antonites, A., 2013. Archaeological evidence for salt production at the Baleni spring, northeastern South Africa. *South African Archaeological Bulletin* **68**, 105-118.

Bernhard, F.O., 1971. Karl Mauch, African Explorer. Struik, Cape Town.

Deer, W.A., Howie, R.A., Zussman, J., 1997. Rock-forming Minerals Orthosilicates. (Second ed).me 1A. The Geological Society, London.

Eriksson, S.C., 1985. Oscillatory zoning in clinopyroxenes from the Guide copper mine Phalaborwa. *South African American Mineralogist* **70**, 74-79.

Evers, T.M., 1974. Three Iron Age Industrial Sites in the Eastern Transvaal Lowveld. MA thesis. University of the Witwatersrand.

Evers, T.M., 1975. Recent Iron Age research in the eastern Transvaal, South Africa. *South African Archaeological Bulletin* **30**, 71-83.

Evers, T.M., 1981. The Iron Age in the eastern Transvaal. In: Voigt, E.A. (Ed.), Guide to Archaeological Sites in the Northern and Eastern Transvaal. Transvaal Museum, Pretoria, 64-109.

Evers, T.M., van der Berg, R.P., 1974. Ancient mining in southern Africa, with reference to a copper mine in the Harmony block, north-eastern Transvaal. *Journal of the South African Institute of Mining and Metallurgy* **74**, 217-226.

Evers, T.M., van der Merwe, N.J., 1987. Iron Age ceramics from Phalaborwa, north eastern Transvaal Lowveld, South Africa. *South African Archaeological Bulletin* **42**, 87-106.

Grant, M., Huffman, T.N., 2007. The extractive metallurgy of copper at Iron Age Madikwe. *South African Journal of Science* **103**, 403-408.

Hall, A.L., 1912. Geology of the Murchison Range and District, Union of South Africa. Geological Survey, Memoir 6, Pretoria.

Hall, S., Miller, D., Anderson, M., Boeyens, J., 2006. An exploratory study of copper and iron production at Marothodi, an early 19th century Tswana town, Rustenburg district, South Africa. *Journal of African Archaeology* **4**, 3-35.

Hanekom, H.J., van Staden, C.M., Smit, P.J., Pike, D.R., 1965. The Geology of the Phalaborwa Igneous Complex. Geological Survey of South Africa Memoir 54, Pretoria.

Hanisch, E.O.M., 1974. Copper working in the Messina district. *Journal of the South African Institute of Mining and Metallurgy* **74**, 250-253.

Hauptmann, A., 2007. The Archaeometallurgy of Copper. Evidence from Faynan, Jordan. Springer Verlag, Berlin.

Huffman, T.N., van der Merwe, H.D., Grant, M.R., Kruger, G.S., 1995. Early copper mining at Thakadu, Botswana. *Journal of the South African Institute of Mining and Metallurgy* **95**, 53-61.

Killick, D.J., 1977. An Attempt to Trace the Movement of the Ores in the Transvaal Lowveld by XRF Analysis of Slags. B.A. (Hons) thesis. University of Cape Town.

Killick, D.J., Miller, D.E., 2014. Smelting of magnetite and magnetite-ilmenite iron ores in the northern Lowveld, South Africa, ca. 1000 CE to ca. 1880 CE. *Journal of Archaeological Science* **43**, 239-255.

Mason, R.J., 1968. Transvaal and Natal Iron Age settlement revealed by aerial photography and excavation. *African Studies* **27**, 1-14.

Miller, D.E., 2002. Smelter and smith: metal fabrication technology in the southern African early and late iron age. *Journal of Archaeological Science* **29**, 1083-1131.

Miller, D., 2010. Indigenous metal melting and casting technology in southern Africa. *South African Archaeological Bulletin* **65**, 45-57.

Miller, D.E., Hall, S., 2008. Rooiberg revisited - the analysis of tin and copper smelting debris. *Historical Metallurgy* **42**, 23-38.

Miller, D.E., Killick, D.J., van der Merwe, N.J., 2001. Metal working in the northern Lowveld, South Africa, AC 1000-1890. *Journal of Field Archaeology* **28**, 401-417.

Miller, D.E., Mulaudzi, M., Killick, D.J., 2002. An historical account of bloomery iron working in the Lowveld, South Africa. *Historical Metallurgy* **36**, 112-121.

Molofsky, L.J., Killick, D.J., Ducea, M.N., Macovei, M., Chesley, J.T., Ruiz, J.,Thibodeau, A.M., Popescu, G.C., 2014. A novel approach to lead isotope provenance studies of tin and bronze: applications to South Africa, Botswanan and Romanian artifacts. *Journal of Archaeological Science* **50**, 440-450.

More, C.E., 1974. Some observations on 'ancient' mining at Phalaborwa. *Journal of the South African Institute of Mining and Metallurgy* **74**, 227-232.

Morimoto, N., Fabries, J., Ferguson, A.K., Ginzburg, I.V., Ross, M., Seifert, F.A., Zussman, J., Aoki, K., Gottardi, G., 1988. Nomenclature of pyroxenes. *American Mineralogist* **73**, 1123-1133.

Palabora Mining Company Geological Staff, 1976. The geology and the economic deposits of copper, iron and vermiculite in the Palabora Igneous Complex. *Economic Geology* **71**, 177-192.

Pearton, T.N., Viljoen, M.J., 1986. Antimony mineralization in the Murchison greenstone belt e an overview. In: Anhaeusser, C.R., Maske, S. (Eds.), Mineral Deposits of South Africa. Geological Society of South Africa, Johannesburg, 293-320.

Pistorius, J., 1989. Die Metaalbewerkers Van Phalaborwa. Ph.D. thesis. University of Pretoria.

Plug, I., Pistorius, J., 1999. Animal remains from industrial Iron Age communities in Phalaborwa, South Africa. *African Archaeological Review* **16**, 155-184.

Schwarz-Shampera, U., Terblanche, H., Oberthür, 2010. Volcanic-hosted massive sulphide deposits in the Murchison greenstone belt, South Africa. *Min. Depos.* **45**, 113-145.

Schwellnus, C.M., 1937. Short notes on the Palaboroa smelting ovens. South Afr. J. Sci. 33, 904-912.

Shand, S.J., 1931. The granite-syenite-limestone complex of Palabora, Eastern Transvaal and the associated apatite deposits. *Transactions of the Geological Society of South Africa* **31**, 81-105.

Stuiver, M., van der Merwe, N.J., 1968. Radiocarbon chronology of the Iron Age in sub-Saharan Africa. *Current Anthropology* **3**, 178-196.

Thondhlana, T.P., 2012. Metalworkers and Smelting Precincts: Technological Reconstructions of Second Millennium Copper Production Around Phalaborwa, Northern Lowveld of South Africa. Ph.D. thesis. University College London.

Thondhlana, T.P., Martinón-Torre, M., Chirikure, S., 2016. The archaeometallurgical reconstruction of early second millennium AD metal production activities at Shankare Hill, northern Lowveld, South Africa. Azania. http://dx.doi.org/10.1080/0067270X.2016.1173309

van der Merwe, N.J., Killick, D.J., 1979. Square: an iron smelting site near Phalaborwa. *South African Archaeological Society, the Goodwin Series* **3**, 86-93.

van der Merwe, N.J., Scully, R.T.K., 1971. The Phalaborwa story: archaeological and ethnographic investigation of a South African Iron Age group. *World Archaeology* **3**, 78-196.

van Eeden, O.R., Kent, L.E., Brandt, J.W., 1939. The Mineral Deposits of the Murchison Range East of Leydsdorp*. Union of South Africa Department of Mines, Memoir* **36**, Pretoria.

van Warmelo, N.J., 1940. The copper Miners of Musina, and the Early History of the Soutpansberg. *Government Printer Ethnographical Publications* **8**, Pretoria.

Verwoerd, W.J., 1956. Sekere produkte van primitiewe koper-, yster-, en bronssmeltery in Oos Transvaal met besonder verwysing na Phalaborwa. Tegnikon 9, 91-104.

Verwoerd, W.J., 1986. Mineral deposits associated with carbonatites and alkaline rocks, In: Anhaeusser, C.R., Maske, S. (Eds.), Mineral Deposits of South Africa. Geological Society of South Africa, Johannesburg, 2173-2191.

Verwoerd, W.J., du Toit, M.C., 2006. The Phalaborwa and Schiel complexes. In: Johnson, M.R., Anhaeusser, C.R., Thomas, R.J. (Eds.), The Geology of South Africa. Council for Geoscience, Pretoria, 291-299.

Viljoen, M.J., Reimold, W.U., 1999. An Introduction to South Africa's Geological and Mining Heritage. Mintek, Randburg.

Wu, F.Y., Yang, Y.-H., Li, Q.L., Mitchell, R.H., Dawson, J.B., Brandl, G., Yuhara, M., 2011. In-situ determination of U-Pb ages and Sr-Nd-Hf isotopic constraints on the petrogenesis of the Phalaborwa carbonatite complex. *South Afr. Lithos.* **127**, 309-322

FIGURES
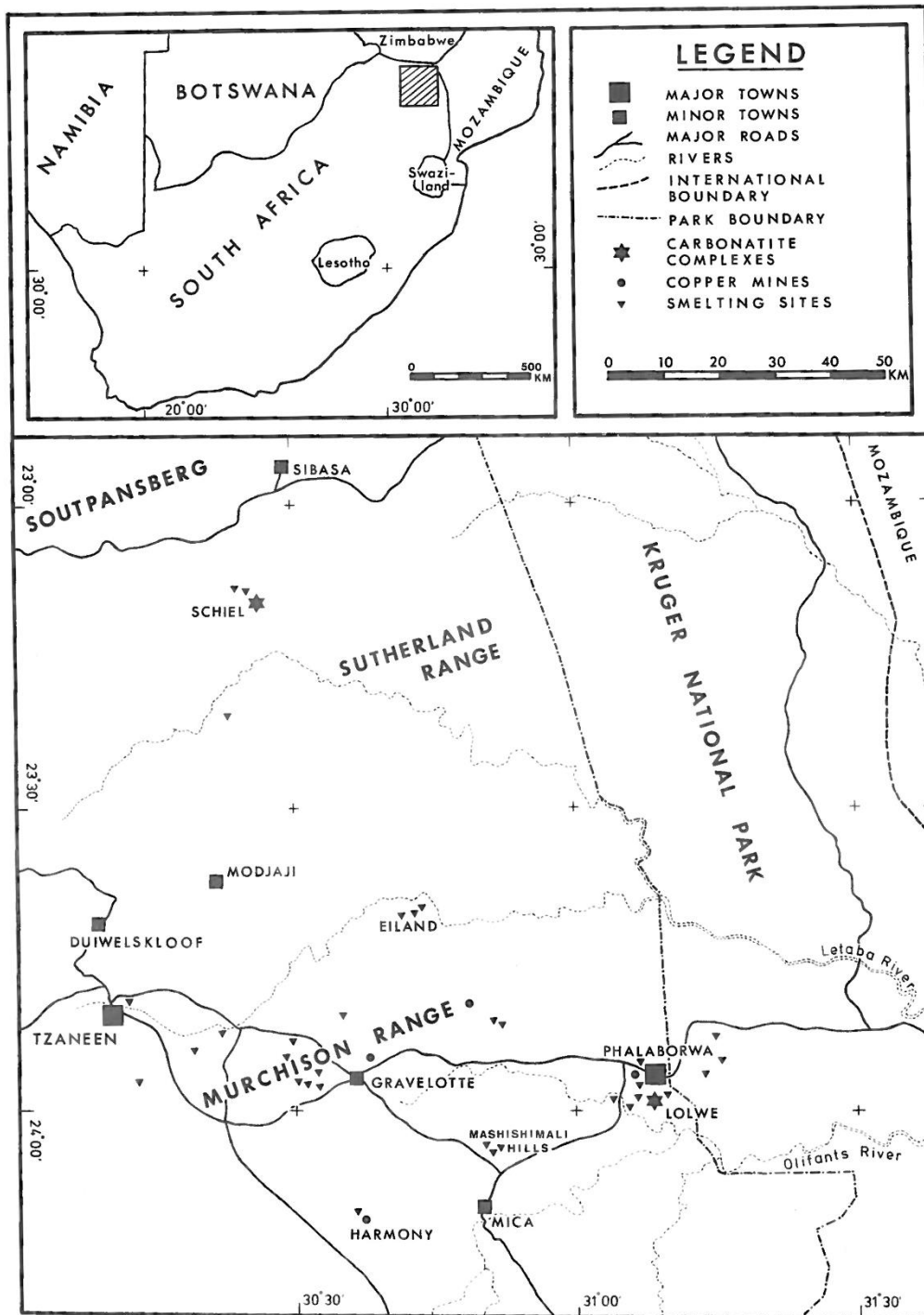
Figure 1. Map of the northern Lowveld, showing principal towns and locations mentioned in this paper.
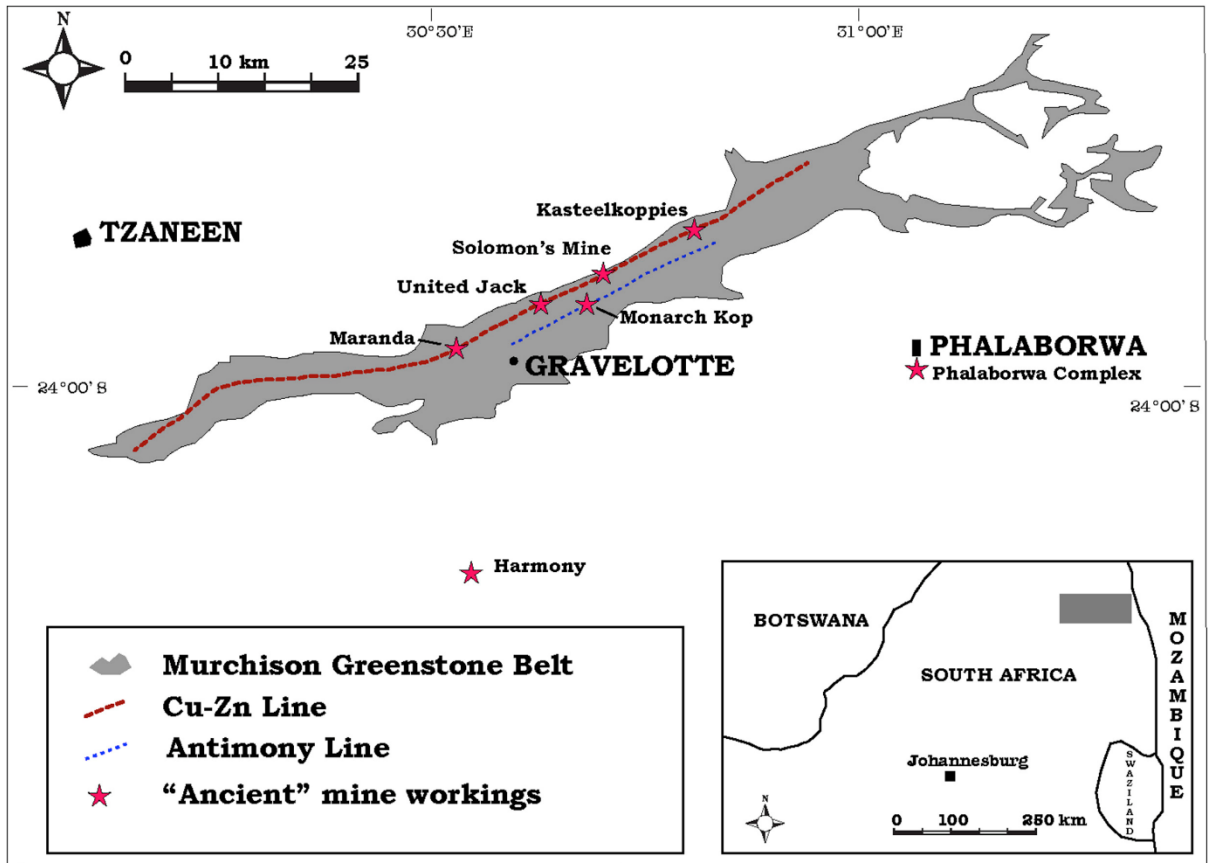
Figure 2. Location of the Murchison Range and the Phalaborwa Carbonatite Complex with respect to the towns of Tzaneen, Gravelotte and Phalaborwa. The outline of the Murchison Greenstone Belt and the Cu-Zn and Antimony Lines are after Schwartz-Shampera et al. (2010: Fig. 1). Locations of 'ancient workings' in the Murchison are transferred from the geological map of van Eeden et al. (1939).
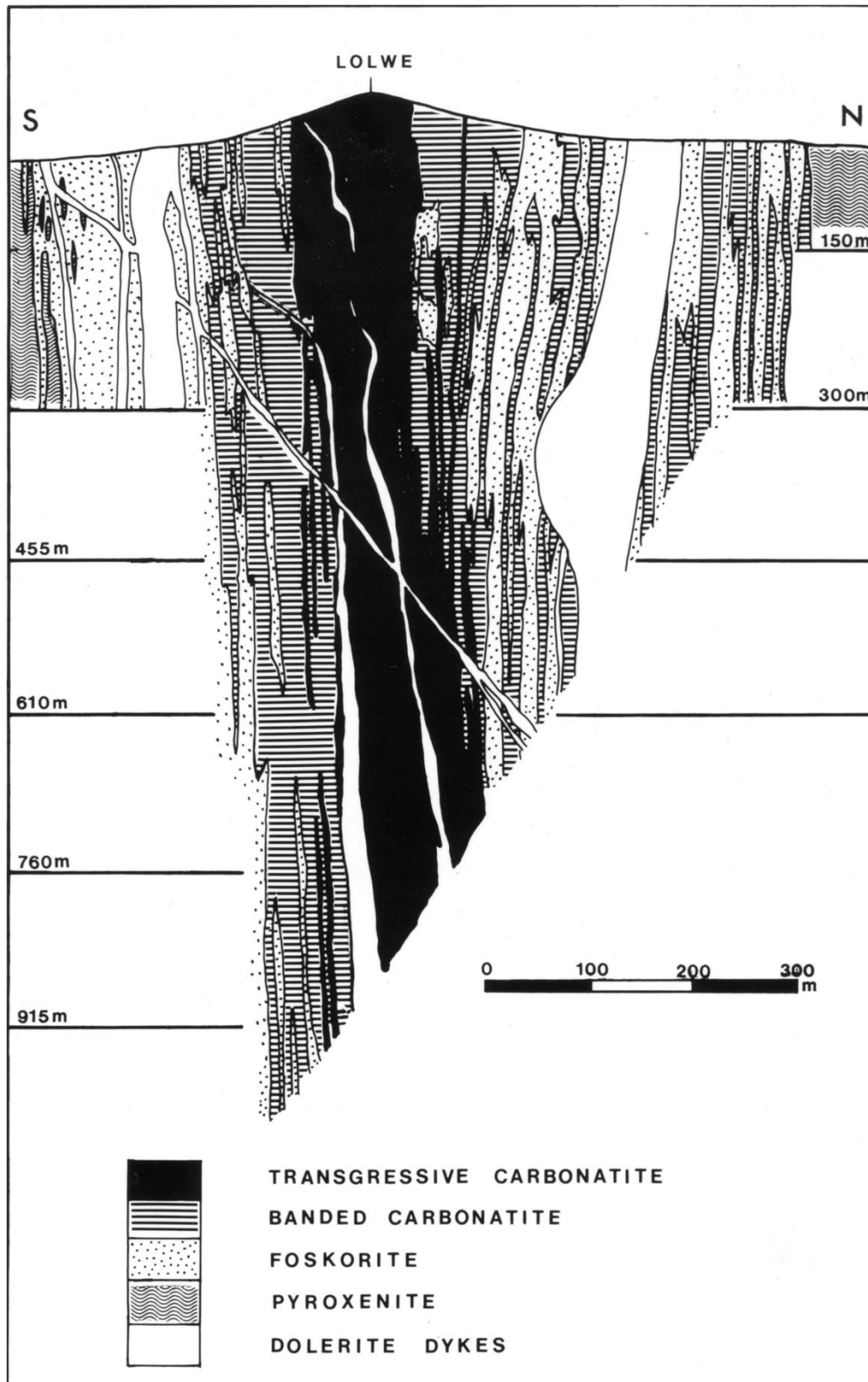
Figure 3. Vertical geological section, defined by drill cores, of the central volcanic pipe of the Phalaborwa Complex before open-pit mining began in 1965. (Redrawn after Palabora Mining Company Geological Staff (1976: Fig. 2)).
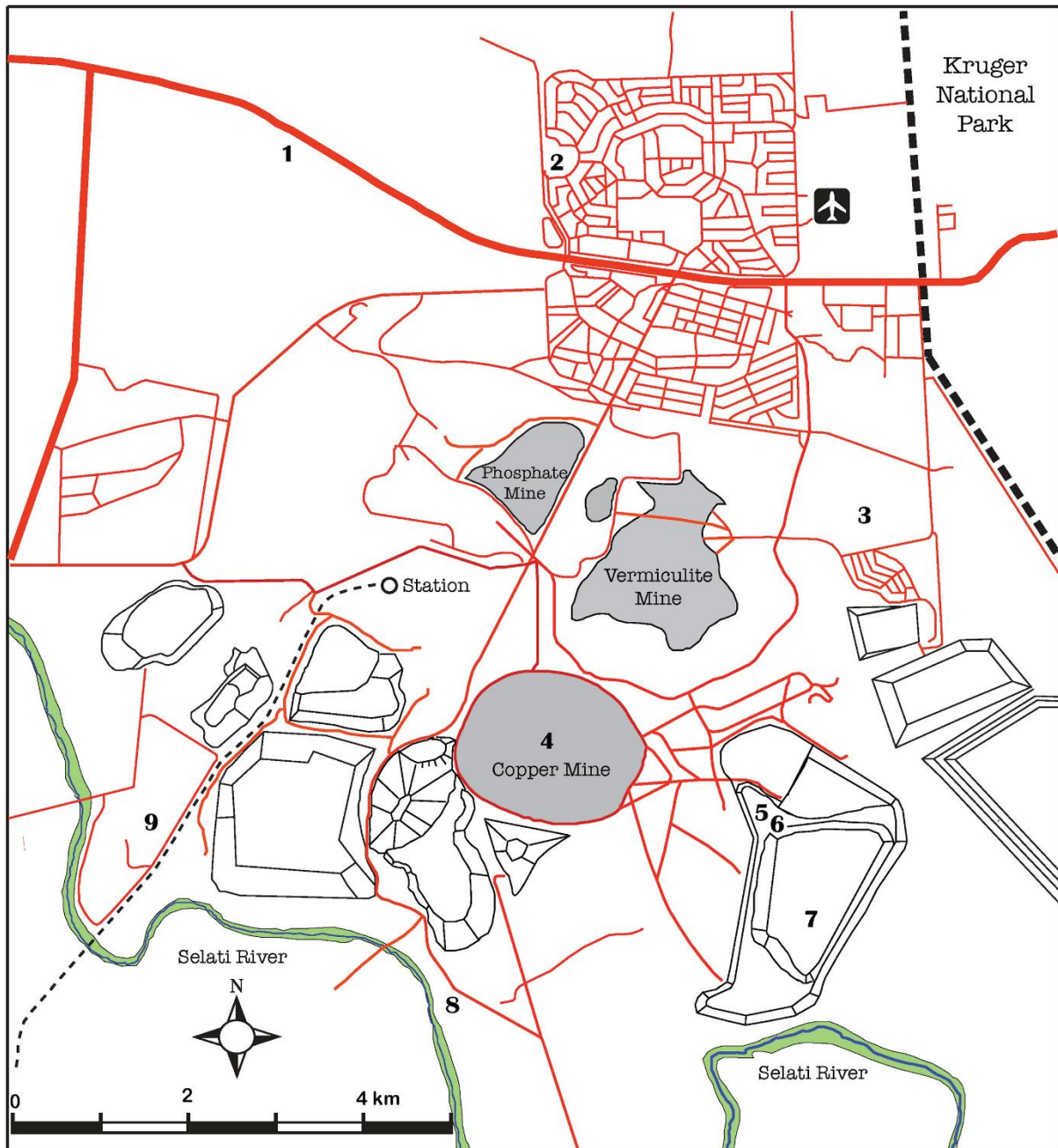
Figure 4. Locations of sites relative to Phalaborwa street grid and the modern mining complex. 1 - Old Guide Mine; 2 - Kgopolwe; 3 - Shankare; 4 - former summit of Lolwe Hill; 5 - Nagome; 6 - Kal; 7 - Molotho; 8 - April Kop; 9 - Serotwe (Matsepe). The base map was scanned from the South African 1987 series 1:50,000 map sheets 2431CC Phalaborwa and 2431AA Grietje. The black-line geometric figures around the mines are heaps of waste rock; these cover the sites labelled 5, 6 and 7.
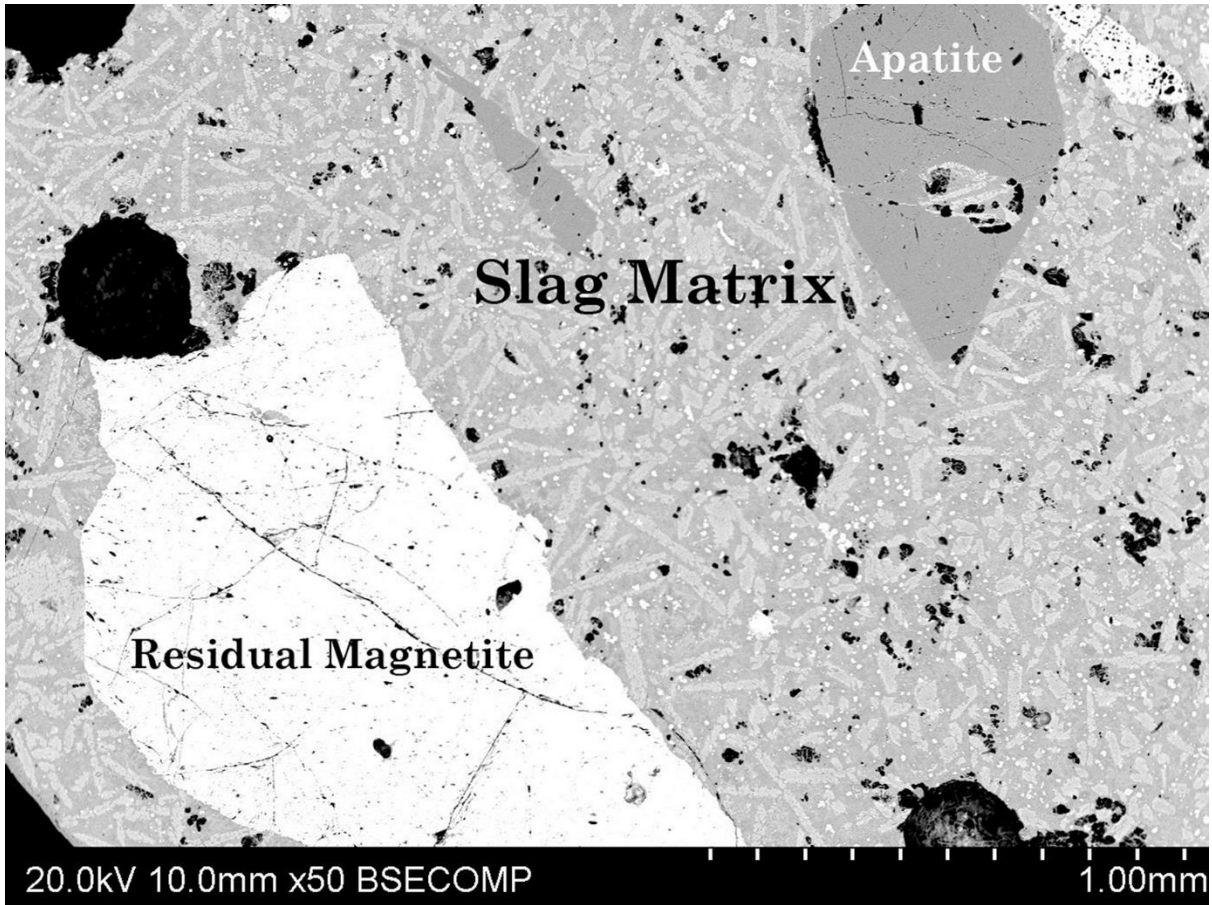
Figure 5. Backscattered SEM image of slag SHA8NWL showing undissolved magnetite and apatite grains.
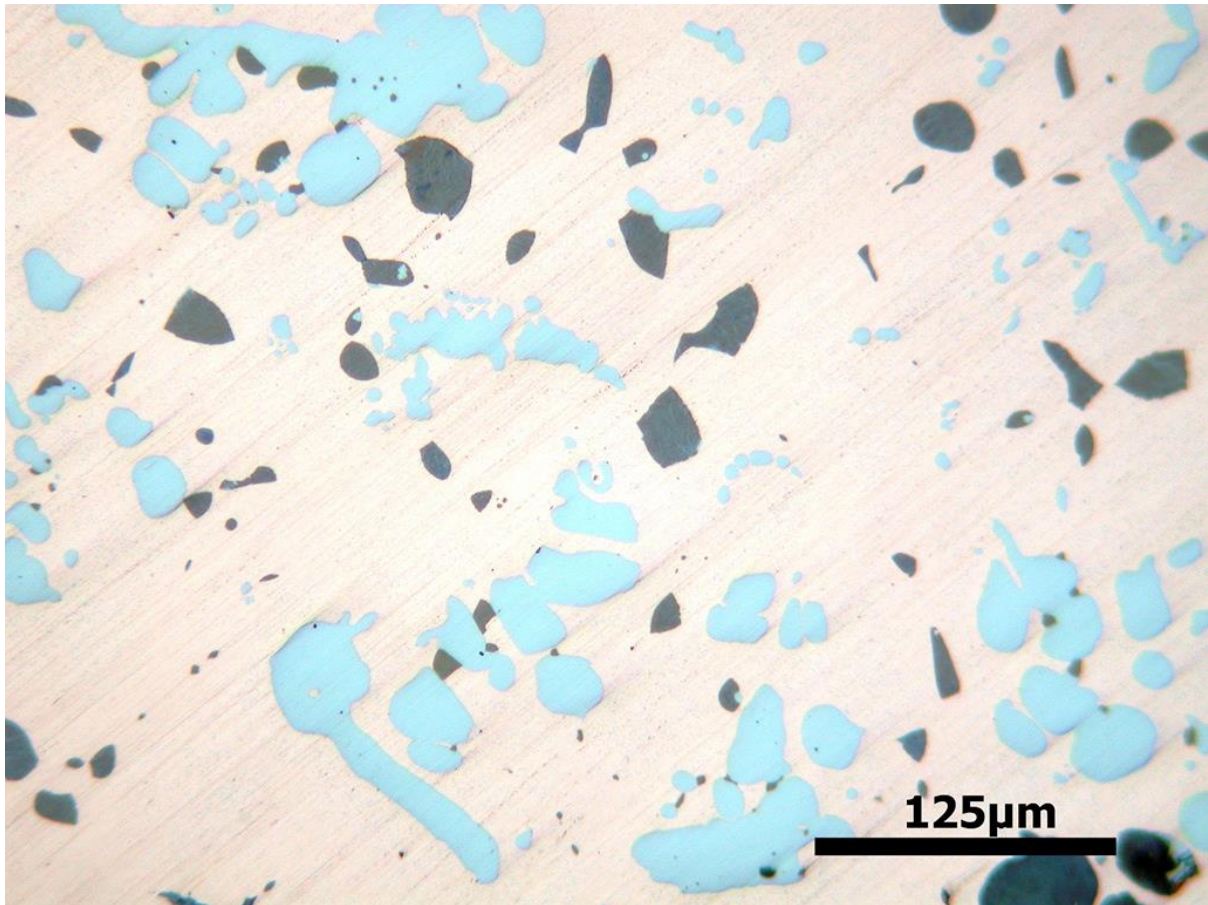
Figure 6. Microstructure of a copper prill in slag sample SHAM18 (Shankare). The light grey inclusions (light blue in pdf version) are metallic iron; the dark grey inclusions are sulphides. Illumination: reflected plane polarised light (PPL). (For interpretation of the references to colour in this figure legend, the reader is referred to the web version of this article.)
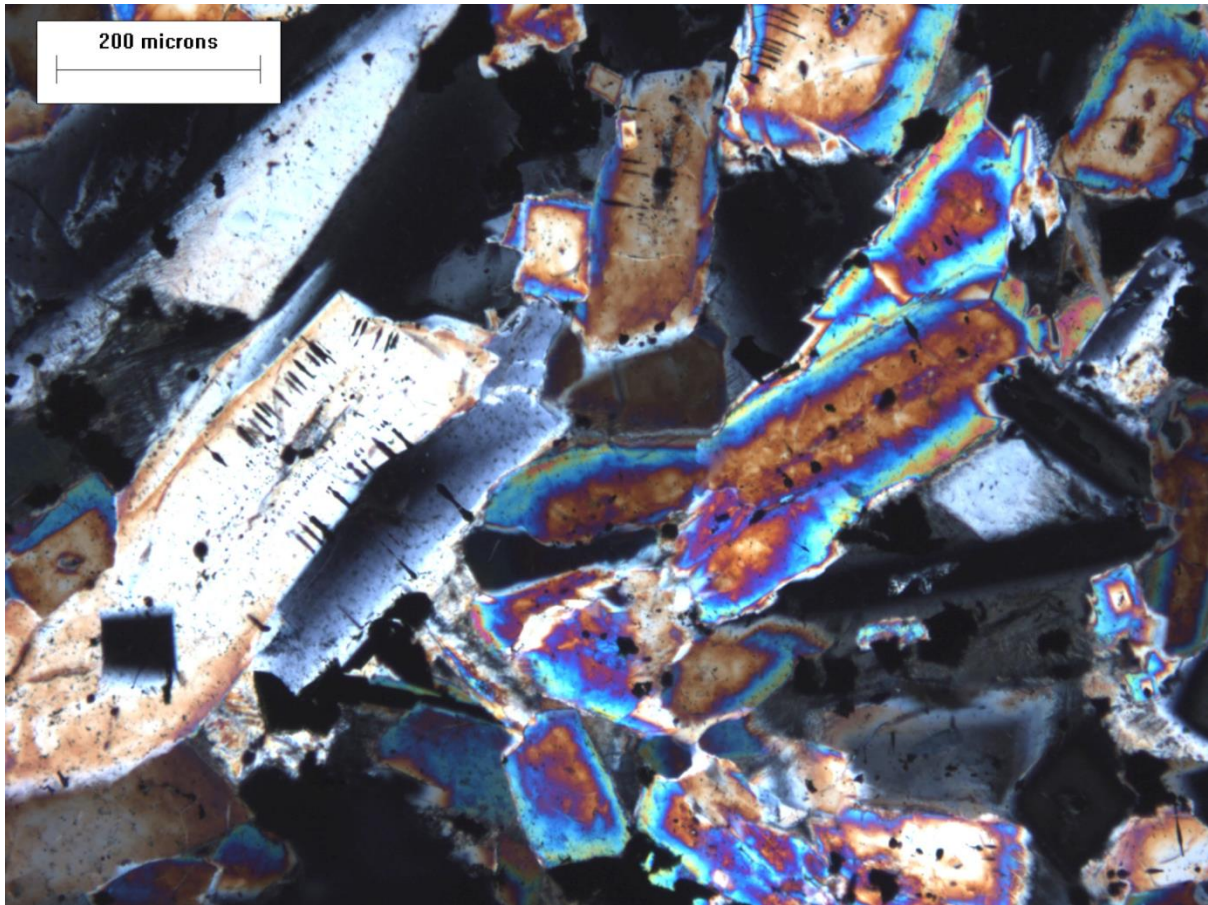
Figure 7. Copper slag from Molotho. The crystals at left with very low birefringence and classic 'peg structure' are melilite. The zoned crystals in the right half have cores of monticellite and rims of kirschsteinite (see Table 6). The opaque rhombs are magnetite. Illumination: transmitted crossed polarised light (XPL).
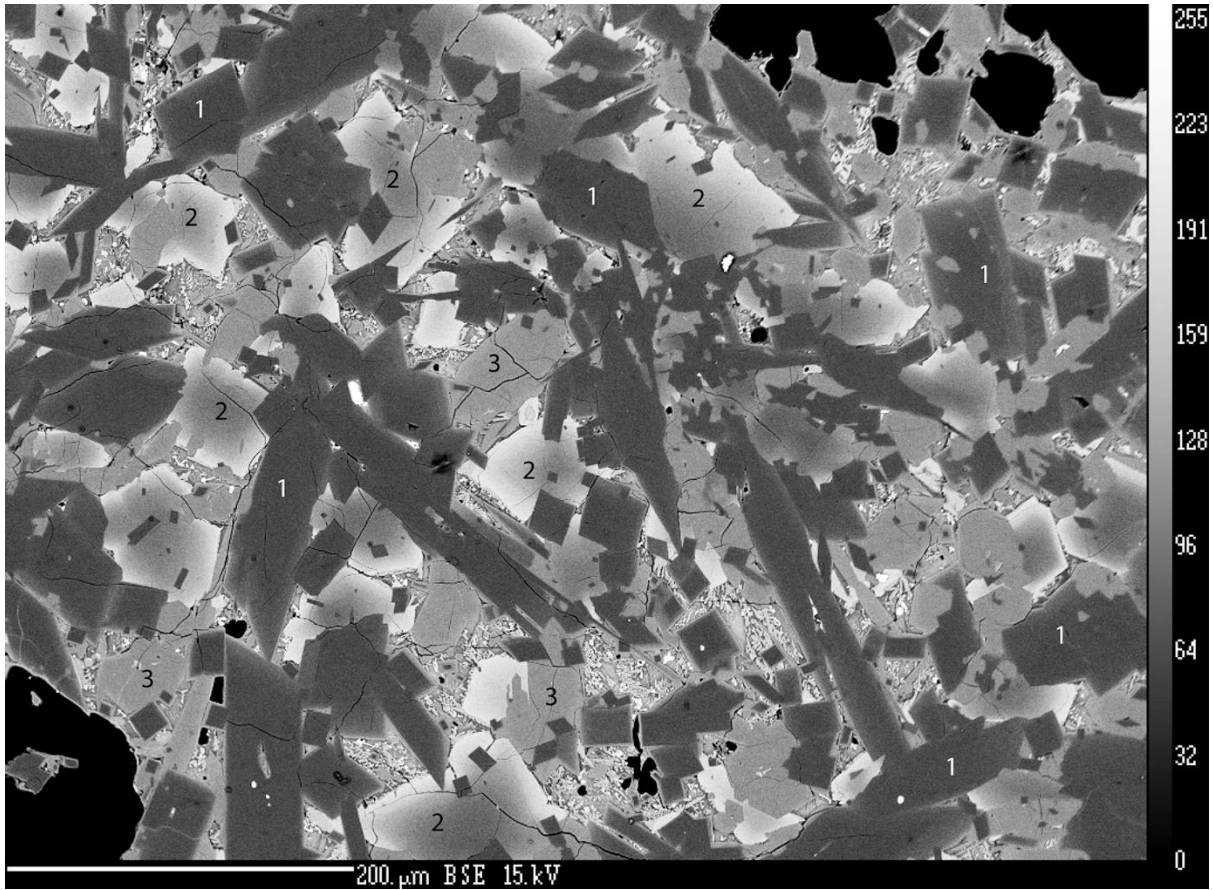
Figure 8. Backscattered SEM image of a polished thin section from SPK4. Phase 1 is a clinopyroxene (diopside). Phase 2 is zoned olivine, with Fe-rich rims. Phase 3 is calcium phosphate. Tiny white crystals of magnetite in glass mark the last stage of solidification of the melt. The black areas are voids.
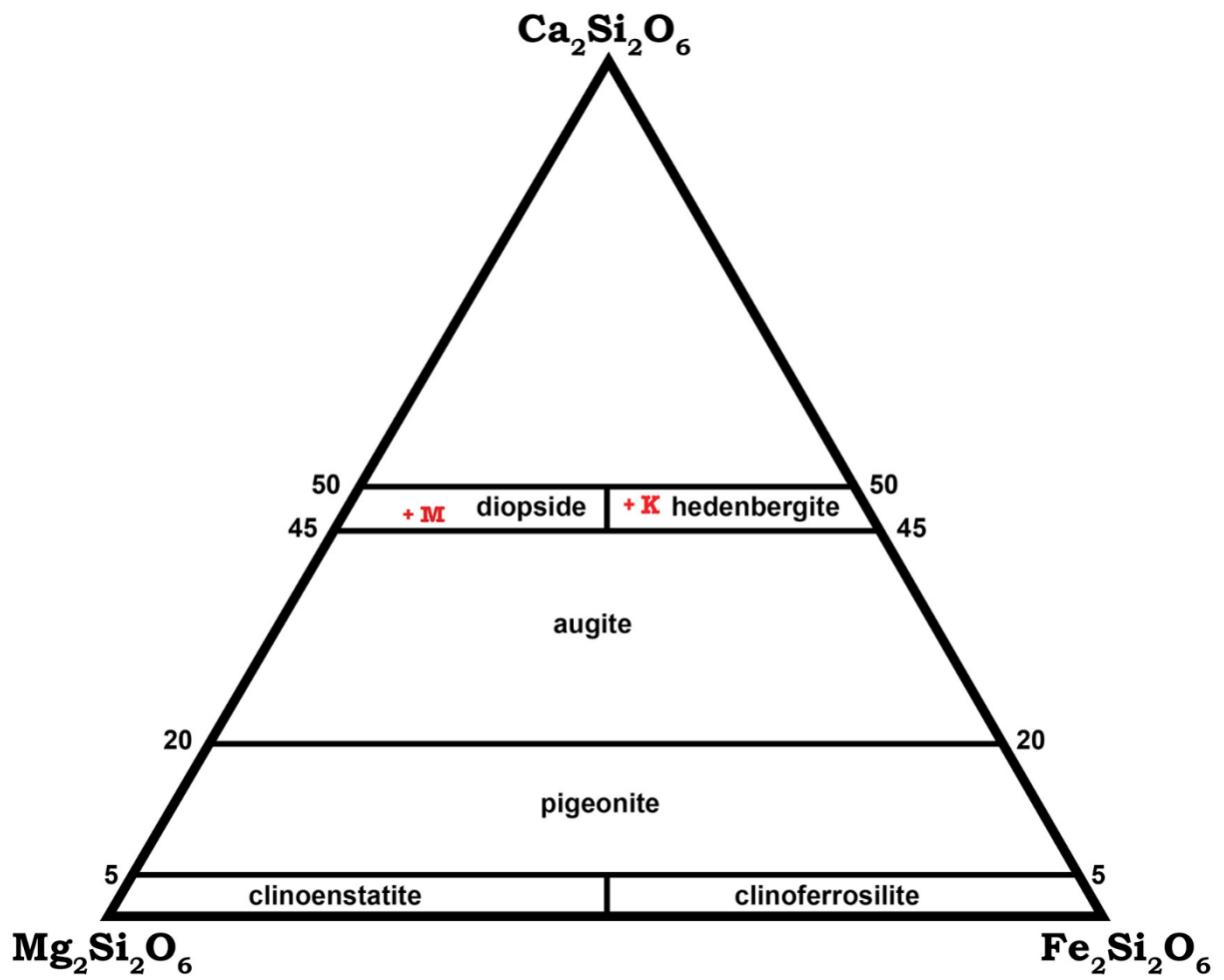
Figure 9. Average composition of pyroxenes in sample SPK-4 (plotted as + K) and SPM-1 (plotted as + M) on the defined compositional fields of the Ca-Mg-Fe clinopyroxenes, redrawn after Morimoto et al. (1988: Fig. 4).
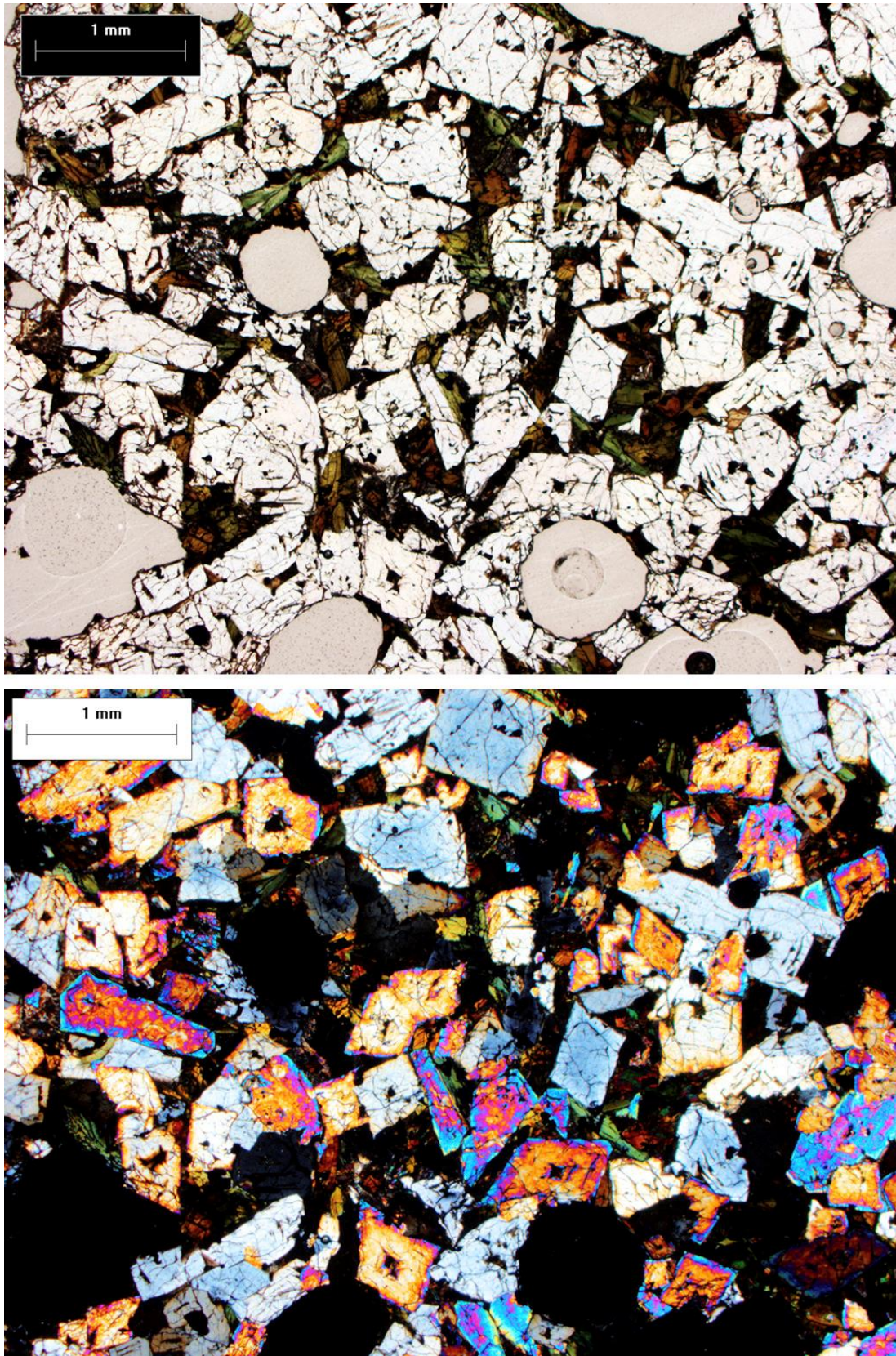
Figure 10. a. Copper slag SPM1 in transmitted PPL showing colourless monticellite and melilite with darker interstitial pyroxene (pleochroic from brown to green). The rounded grey areas are trapped gas bubbles. b. Same field of view in transmitted XPL. The crystals showing uniform colour (white to light grey) are melilites; those showing zoning of rims and higher birefringence are ferroan monticellites. (For interpretation of the references to colour in this figure legend, the reader is referred to the web version of this article.)

TABLES

Table 1. Radiocarbon dates for copper mines, copper furnaces and habitation sites with copper objects in the northern Lowveld. The calibrated age ranges were obtained with Calib 7.0, using the SHCal13 curve (http://calib.qub.ac.uk/calib/calib.html).

Site	Sample	^{14}C yrs BP	Calibrated at 2 σ (% probability).	Context
Lolwe mine	Y-1636	1180 ± 80	681–746 (6.7%), 756–1033 (93.3%)	mine gallery
Lolwe mine	Y-1635	950 ± 60	1020–1229 (99.1%), 1251–1260 (9%)	mine gallery
Lolwe mine	GrN-4215	160 ± 30	1673–1742 (30.0%), 1772–1777 (6.0%), 1797–1950 (69.5%)	mine adit
Harmony mine	RL-207	690 ± 90	1220–1437 (100%)	mine dump
Shankare (SHA2M1)	Pta-4443	890 ± 50	1046–1089 (10.6%), 1108–1121 (1.6%), 1129–1277 (87.8%)	copper furnace
Shankare (SHAM1)	Beta-306714	830 ± 30	1206–1283 (100%)	midden
Shankare (SHAM1)	Beta-306715	840 ± 30	1189–1194 (1.1%), 1196–1279 (98.9%)	midden
Shankare (SHAM1)	Beta-306716	1010 ± 30	1022–1151 (100%)	midden
Kgopolwe (SPK3)	Y-1639	850 ± 60	1046–1087 (4.9%), 1113–1116 (0.2%), 1133–1300 (94.6%), 1367–1373 (0.3%)	house floor
Kgopolwe (SPK3)	Y-1637	910 ± 60	1040–1269 (100%)	house floor
Kgopolwe (SPK3)	Y-1662	820 ± 80	1046–1088 (5.0%), 1110–1118 (0.5%), 1131–1327 (85.3%), 1339–1390 (9.2%)	house floor
Kgpolwe (SPK4)	Y-1657	520 ± 60	1318–1353 (5.4%), 1384–1508 (89.5%), 1583–1620 (5.2%)	slag heap
Matsepe (SPM1)	Y-1660	80 ± 60	1650–1950	copper furnace
Molotho (MOL1)	Y-1661	60 ± 120	1650–1950	copper furnace
Nagome (MN1)	Pta-567	110 ± 40	1650–1950	copper furnace

Table 2. SEM-EDS 'bulk' analyses of ore samples from Shankare and Kgopolwe.

Site	Sample	Context	Na$_2$O	MgO	Al$_2$O$_3$	SiO$_2$	P$_2$O$_5$	SO$_3$	K$_2$O	CaO	TiO$_2$	MnO	FeO	CuO	BaO	Total
SHANKARE	SHA1T	surface	0.0	0.3	0.1	1.3	6.0	0.1	0.0	18.3	0.0	0.1	16.7	12.7	0.0	55.7
SHANKARE	SHA2NWL	surface	0.0	10.5	0.0	42.8	0.7	1.2	0.1	13.5	0.1	0.1	4.5	22.2	1.9	97.7
SHANKARE	SHA11NEL	surface	0.0	0.1	0.1	2.3	0.5	1.1	0.0	2.4	0.0	0.0	34.1	35.9	0.1	76.7
SHANKARE	SHA12NEL	surface	0.0	0.2	0.1	1.5	0.3	0.2	0.0	16.4	0.0	0.1	20.4	29.7	0.0	69.0
SHANKARE	SHA13NEL	surface	0.0	0.2	0.2	0.7	0.3	0.1	0.0	0.1	0.1	0.0	8.3	59.6	0.0	69.5
SHANKARE	SHA14NEL	surface	0.0	0.1	0.1	0.8	0.2	0.1	0.0	9.8	0.1	0.0	11.0	45.6	0.0	67.9
SHANKARE	SHA15NEL	surface	0.0	0.4	0.6	2.1	0.3	0.0	0.0	1.0	0.0	0.1	0.3	57.9	0.1	62.7
SHANKARE	SHA16NEL	surface	0.0	0.3	0.1	1.3	0.2	4.5	0.0	0.2	0.1	0.1	4.4	54.7	0.1	66.0
SHANKARE	SMB22(4)	SHAM1	0.0	1.4	1.3	1.2	0.3	0.0	0.0	0.4	0.0	0.1	62.8	7.5	0.0	75.2
SHANKARE	SMB22(5)	SHAM1	0.0	2.4	0.1	7.1	0.8	1.6	0.0	2.8	0.0	0.1	25.4	29.9	0.0	70.1
SHANKARE	SMB26(2)	SHAM1	0.0	0.1	0.0	45.0	0.1	0.1	0.0	0.6	0.0	0.0	14.5	28.0	0.0	88.5
SHANKARE	SMB26(3)	SHAM1	0.0	0.2	0.1	3.1	0.0	0.2	0.0	0.2	0.0	0.1	27.9	27.2	0.0	59.0
SHANKARE	SMB26(4)	SHAM1	0.0	6.0	2.1	6.4	0.2	0.0	0.0	0.7	0.0	0.0	1.1	56.2	0.0	72.7
SHANKARE	SMB27(1)	SHAM1	0.0	0.3	0.2	1.2	0.1	2.5	0.0	4.4	0.0	0.0	6.2	52.7	0.0	67.6
KGOPOLWE	SPK3.1	SPK3	0.0	0.1	0.0	4.4	0.1	11.3	0.0	0.2	0.0	0.0	41.5	22.9	0.9	81.5
KGOPOLWE	SPK3.2	SPK3	0.0	0.3	0.1	7.5	0.9	1.9	0.0	0.3	0.0	0.0	29.4	32.6	0.2	73.1
maximum			0.0	10.5	2.1	45.0	6.0	11.3	0.1	18.3	0.1	0.1	62.8	59.6	1.9	
minimum			0.0	0.1	0.0	0.7	0.0	0.0	0.0	0.1	0.0	0.0	0.3	7.5	0.0	

Table 3. SEM-EDS averaged 'bulk' analyses of copper slags from Phalaborwa.

Site/Sample	Context	Na$_2$O	MgO	Al$_2$O$_3$	SiO$_2$	P$_2$O$_5$	SO$_3$	K$_2$O	CaO	TiO$_2$	MnO	FeO	CuO	Sum
SHANKARE														
SHA1NWL	surface	0.5	10.2	0.8	51.4	4.7	0.1	0.7	24.9	0.4	0.1	5.8	0.3	99.9
SHA4NWL	surface	0.4	4.2	3.2	35.2	5.7	0.1	1.1	18.8	0.5	0.1	30.3	0.3	99.9
SHA5NWL	surface	0.5	4.1	3.1	34.7	5.9	0.0	1.2	17.4	0.7	0.2	31.5	0.6	99.9
SHA6NWL	surface	0.5	3.7	3.7	35.1	4.9	0.1	1.3	18.9	0.6	0.2	30.8	0.3	100.1
SHA7NWL	surface	0.3	5.6	2.4	33.0	4.5	0.0	0.8	17.0	0.5	0.2	35.4	0.3	100.0
SHA8NWL	surface	0.5	3.5	3.1	34.7	6.2	0.1	1.0	19.3	0.7	0.2	29.9	0.7	99.9
SHA9NEL	surface	0.5	6.0	2.3	34.3	3.3	0.1	0.8	26.6	0.5	0.2	24.9	0.5	100.0
SHA9NWL	surface	0.5	3.4	3.1	34.6	0.9	0.1	0.9	14.7	0.3	0.1	40.4	1.0	100.0
SHA10NEL	surface	0.7	2.9	3.1	30.4	12.4	0.1	1.0	16.8	0.9	0.3	29.5	2.1	100.2
SHA10NWL	surface	0.4	3.7	3.4	36.1	4.6	0.0	1.3	18.0	0.6	0.1	30.8	0.8	99.8
SHAMK7(1)	Scatter 7	0.5	3.8	3.1	30.0	1.9	1.5	1.4	28.1	0.2	0.2	29.0	0.4	100.1
SHAMK7(2)	Scatter 7	0.4	6.6	2.8	32.3	1.8	0.2	0.9	25.9	0.1	0.3	28.3	0.5	100.1
SHAMK7(3)	Scatter 7	0.2	5.7	1.2	30.7	1.5	0.1	0.4	17.8	0.1	0.3	40.0	1.8	99.8
SHAMK8(1)	Scatter 8	0.2	5.8	2.1	32.6	4.7	0.1	0.5	22.1	0.5	0.2	29.2	2.0	100.0
SHAMK9(1)	Scatter 9	0.7	3.4	3.2	32.1	1.7	0.1	1.0	14.8	0.6	0.1	41.5	1.0	100.2
SHAMK18(1)	Scatter 18	0.1	5.3	1.1	42.7	1.7	0.0	0.3	17.2	0.5	0.3	27.9	2.9	100.0
SHAMK18(2)	Scatter 18	0.2	6.9	1.6	40.6	1.7	0.1	0.5	22.7	0.3	0.3	24.0	1.2	100.1
SHAMK18(3)	Scatter 18	0.5	3.4	3.2	31.7	3.6	0.2	0.8	15.6	0.1	0.2	39.8	0.9	100.0
SHAMK18(4)	Scatter 18	0.3	1.4	1.8	37.3	4.3	0.0	0.7	8.2	0.3	0.2	45.0	0.5	100.0
SHAMK27(3)	Scatter 27	0.4	3.4	2.4	36.6	0.9	0.0	0.7	9.0	0.3	0.2	43.9	2.2	100.0

SHARS(2)	roadside	0.2	4.7	2.1	34.7	7.8	0.1	0.5	21.3	0.5	0.2	26.7	1.3	100.1
SMB21(1)	SHAM1	0.3	5.6	1.6	32.1	1.1	0.2	0.7	13.8	0.2	0.3	41.4	2.7	100.0
SMB22(1)	SHAM1	0.3	2.7	2.5	36.3	0.8	0.2	0.9	9.6	0.2	0.1	44.8	1.6	100.0
SMB22(2)	SHAM1	0.3	5.1	2.6	31.8	1.0	0.6	0.6	21.4	0.4	0.2	34.6	1.4	100.0
SMB23(1)	SHAM1	0.5	4.5	2.6	34.5	0.7	0.3	0.9	19.8	0.3	0.2	34.7	1.1	100.1
SMB24(1)	SHAM1	0.2	3.6	1.2	28.9	0.9	0.1	0.3	18.4	0.2	0.2	43.9	2.1	100.0
SMB26(1)	SHAM1	0.3	3.0	2.2	38.4	3.5	0.0	0.6	23.1	0.4	0.2	27.2	1.0	99.9
MOLOTHO														
MOL1F	furnace	0.2	11.6	0.7	39.0	1.1	0.0	0.6	26.1	0.2	0.2	17.6	2.6	99.9
MOL2F	furnace	0.2	10.8	0.7	38.4	1.1	0.1	0.7	26.5	0.3	0.1	17.8	3.3	100.0
MOL3F	furnace	0.1	1.9	0.2	46.2	1.2	0.0	0.5	22.9	0.4	0.3	22.1	4.1	99.9
MOL4F	furnace	0.1	9.2	0.2	36.2	1.1	0.1	0.4	24.0	0.1	0.3	23.1	5.3	100.1
MOL5F	furnace	0.3	7.8	0.7	33.2	0.7	0.2	1.0	23.6	0.3	0.3	31.3	0.8	100.2
MOL6F	furnace	0.2	8.7	1.4	40.2	0.8	0.1	0.9	23.1	0.2	0.2	23.2	1.0	100.0
KGOPOLWE														
SPK 3	ingot slag	0.0	3.5	1.7	27.2	1.6	0.0	0.2	6.9	1.2	0.3	55.7	1.8	100.1
SPK 3.10a	slag in pot	0.0	0.6	6.1	21.2	0.0	0.0	1.8	3.2	0.8	0.0	66.3	0.0	100.0
SPK 3.10a	slag in pot	0.0	1.0	7.8	26.6	0.8	0.0	2.0	4.1	0.5	0.0	57.1	0.3	100.2
SPK 3.13	Unit 12	0.0	5.3	2.5	29.8	3.1	0.5	0.6	24.9	0.0	0.0	25.5	7.9	100.1
MATSEPE/SEROTWE														
SPM1(1)	slag heap	0.3	6.4	1.2	40.7	0.6	0.1	0.4	19.9	0.2	0.2	28.5	1.5	100.0
SPM1(2)	slag heap	0.0	3.6	0.6	39.7	0.4	0.1	0.3	14.9	0.3	0.2	38.1	1.8	100.0
SPM1(3)	slag heap	0.4	6.1	1.1	45.8	0.6	0.1	0.5	19.2	0.2	0.2	22.0	3.8	100.0
SPM1(4)	slag heap	0.3	5.7	1.2	44.9	0.7	0.0	0.5	19.0	0.2	0.1	23.3	4.2	100.0

Table 4. Chemical analyses of powdered bulk samples of copper slags from Phalaborwa. The analyses for Matsepe and Kgopolwe were made by WD-XRF on glass discs; the other analyses are from Pistorius (1989), did not report the technique used to obtain them. Blank cells denote that the concentration of that element was not measured.

Site	Sample	SiO_2	TiO_2	Al_2O_3	Fe_2O_3	FeO	MnO	MgO	CaO	Na_2O	K_2O	P_2O_5	CO_2	H_2O+	H_2O-	Cu met. %	Sum
Matsepe	SPM1a	38.34	4.84	7.89	6.21	27.79	0.21	2.75	6.81	1.29	2.22	0.38	0.30	0.30	0.07	0.45	99.85
Kgopolwe	SPK3.10	13.77	1.11	3.38	15.48	56.28	0.23	0.82	3.09	0.84	0.96	0.23			0.07	0.09	96.35
Shankare	SHA2M1	50.20		5.30	18.50			4.10	15.00	0.60	1.80					1.07	96.57
Shankare	SHA1T18	56.40		6.40	11.50			4.20	13.20	0.80	2.50					0.68	95.68
Pjenne	Furnace 1	40.10		2.80	25.70			5.80	21.20	0.10	0.60					1.70	98.00
Mapotini	MAP2	42.10		4.40	25.80			3.00	17.60	0.30	1.30					1.33	95.83
Mapotini	MAP3	44.10		5.60	23.90			2.70	15.50	0.50	1.90					0.61	94.81
Marupale	Blok A	43.50		3.00	20.20			5.90	24.60	0.10	0.60					2.50	100.4
Marupale	Blok B	44.60		3.10	16.90			4.70	29.10	0.10	0.70					1.77	100.97
Marupale	MAR3T6	43.60		2.90	21.40			5.70	24.20	0.10	0.50					1.96	100.36
Marupale	MAR3T3	49.20		2.80	16.10			2.50	28.10	0.10	0.50					2.18	101.48
Ghoenkop	GH2M1	45.30		3.40	12.40			6.10	32.10	0.10	1.00					1.25	101.65
Ghoenkop	GH1T3-1	49.50		3.40	8.40			8.10	19.80	0.40	1.40	3.00				1.20	95.20
Ghoenkop	GH1T3-2	51.50		2.70	7.90			9.40	21.00	0.40	0.90	2.90				1.10	97.80
Ghoenkop	GH1T3-3	50.00		2.70	7.60			9.20	21.50	0.40	0.80	3.00				2.20	97.40
Sonkanini	SON2M1	51.20		4.00	16.10			5.60	17.20	0.40	1.00					2.12	97.62
Evkomkop	buite	62.90		8.20	11.20			1.70	9.60	1.40	2.00					0.69	97.69
Evkomkop	EVKL2	48.70		3.10	12.80			5.00	23.30	0.10	0.70	1.10				1.00	95.80
Evkomkop	EVKL3	46.40		3.80	13.60			6.20	24.70	0.30	0.90	1.10				1.8	98.80

Table 5. SEM-EDS analyses of silicate mineral crystals in slags from Phalaborwa sites, in wt%, normalised to 100%.

Analysis	Sample	Phase	SiO_2	TiO_2	Al_2O_3	FeO	MnO	MgO	CuO	CaO	Na_2O	K_2O	P_2O_5	Total
1	MOL1F	melilite?	45.2			4.0		11.8		39.0				100.0
2	MOL2F	melilite	39.8			8.7		19.2		32.3				100.0
3	MOL3F	wollastonite?	53.7			8.7		2.8		34.8				100.0
4	MOL4F	?	46.5			7.2		11.7		34.6				100.0
5	MOL5F	monticellite	37.0			17.9		14.6		30.5				100.0
6	MOL6F	monticellite	36.6			22.5		13.5		27.5				100.0
7	SPK3.10	glass	40.4	0.5	20.5	15.1				9.7	5.9	6.4	1.5	100.0
8	SPK3.10	glass	44.4	0.1	19.9	15.9				9.3	0.9	7.5	2.0	100.0
9	SPK3.10	fayalite	32.2			63.1		2.6		2.1				100.0
10	SPK3.10	wüstite	0.8	1.4	1.3	96.5								100.0
11	SPK3.13	glass	66.4	0.7	9.9	9.2		1.2	1.6	5.1		2.2	3.7	100.0
12	SPK3.13	melilite?	44.3			13.9		11.2		28.9			1.7	100.0
13	SPK3.13	glass	33.2		4.6	18.6			5.9	29		1.4	7.3	100.0

14	SPM1	monticellite?	35.2			31.9		7.6		25.3				100.0
15	SPM1	kirschsteinite	33.6			53.2		3.7		9.5				100.0
16	SPM1	hedenbergite	48.8			19.5		8.7		23				100.0
17	SPM1	hedenbergite	48.2			21.2		8.0		22.6				100.0

Table 6. Electron microprobe analyses (wt%) of silicate crystals in a thin section of a slag from Molotho hill. na – not analysed.

Analysis	Phase		SiO$_2$	TiO$_2$	Al$_2$O$_3$	FeO	MnO	MgO	CaO	K$_2$O	Na$_2$O	Cr$_2$O$_3$	CuO	P$_2$O$_5$	SrO	Total
1	melilite		42.06	0.00	0.60	5.13	0.09	11.07	39.44	0.12	0.06	0.00	0.05	0.01	na	98.63
2	melilite		41.75	0.01	0.64	5.16	0.06	10.91	38.99	0.20	0.12	0.02	0.14	0.09	na	98.10
3	melilite		42.19	0.01	0.56	5.07	0.09	11.00	39.32	0.12	0.08	0.01	0.07	0.00	na	98.51
4	melilite		41.55	0.02	0.62	5.21	0.05	10.81	39.29	0.15	0.09	0.00	0.05	0.09	na	97.93
5	melilite		41.41	0.02	0.68	5.31	0.06	10.82	39.25	0.18	0.1	0.00	0.04	0.05	na	97.91
6	melilite		41.30	0.00	0.65	5.06	0.08	11.10	39.22	0.22	0.12	0.00	0.18	0.34	na	98.27
7	melilite		40.92	0.02	0.78	6.46	0.06	10.00	38.96	0.21	0.13	0.00	0.06	0.07	na	97.66
8	melilite		41.02	0.01	0.88	6.87	0.09	9.61	38.44	0.33	0.16	0.00	0.12	0.12	na	97.66
9	meliliite		41.58	0.01	0.78	5.23	0.05	10.77	39.11	0.25	0.14	0.00	0.11	0.36	na	98.40
10	melilite		41.58	0.02	0.88	5.47	0.10	10.61	39.31	0.21	0.14	0.00	0.04	0.05	na	98.42
11	melilite		40.98	0.00	0.73	6.46	0.09	10.06	38.88	0.25	0.12	0.00	0.03	0.03	na	97.63
12	melilite		40.83	0.00	0.76	7.86	0.13	9.33	38.57	0.27	0.12	0.00	0.04	0.02	na	97.93
13	melilite		40.59	0.00	0.73	8.38	0.16	8.84	38.26	0.33	0.13	0.00	0.01	0.03	na	97.47
14	melilite		40.59	0.00	0.73	8.38	0.16	8.84	38.26	0.33	0.13	0.00	0.01	0.03	na	97.47
15	melilite		41.01	0.01	0.74	8.00	0.18	9.00	38.45	0.35	0.14	0.01	0.00	0.06	0.51	98.44
16	monticellite	core	35.04	0.00	0.00	15.28	0.26	14.04	34.22	0.00	0.04	0.00	0.16	0.29	na	99.33
17	monticellite	core	34.99	0.02	0.02	13.66	0.20	15.40	34.20	0.00	0.01	0.01	0.06	0.13	na	98.69
18	monticellite	rim	31.41	0.06	0.03	29.50	0.34	2.79	33.54	0.01	0.1	0.04	0.19	0.57	na	98.60
19	monticellite	core	34.54	0.04	0.01	14.27	0.29	14.90	34.33	0.00	0.01	0.01	0.22	0.41	na	99.02
20	monticellite	rim	32.78	0.04	0.01	23.04	0.32	8.03	34.00	0.01	0.07	0.01	0.19	0.41	na	98.93
21	monticellite	rim	31.34	0.06	0.03	28.97	0.34	3.13	33.79	0.02	0.12	0.04	0.16	0.55	na	98.54
22	monticellite	core	34.90	0.00	0.01	11.70	0.27	16.92	34.27	0.01	0.01	0.00	0.18	0.25	na	98.51
23	monticellite	rim	33.00	0.04	0.00	21.51	0.32	9.25	33.98	0.02	0.06	0.01	0.19	0.34	na	98.71
24	monticelliite	core	33.87	0.02	0.02	17.90	0.24	11.87	34.32	0.00	0.07	0.01	0.15	0.33	na	98.82
25	monticelliite	core	34.63	0.02	0.01	16.02	0.29	14.08	34.16	0.00	0.02	0.01	0.17	0.44	na	99.85
26	monticelliite	core	34.43	0.02	0.01	14.85	0.25	14.35	34.49	0.00	0.03	0.00	0.22	0.32	na	98.97
27	monticellite	core	35.16	0.00	0.03	13.79	0.24	15.46	34.06	0.00	0.01	0.00	0.15	0.35	na	99.25
27	magnetite		0.08	0.45	1.52	92.40	0.19	0.59	0.11	na	na	0.05	0.02	na	na	95.40
29	magnetite		0.09	0.33	1.51	91.75	0.20	1.12	0.17	na	na	0.02	0.02	na	na	95.21
30	magnetite		0.08	0.42	1.69	92.07	0.15	0.84	0.20	na	na	0.02	0.04	na	na	95.52
31	magnetite		0.11	0.37	1.65	91.62	0.16	0.57	0.50	na	na	0.03	0.03	na	na	95.05
32	magnetite		0.07	0.72	1.64	92.35	0.17	0.23	0.20	na	na	0.02	0.01	na	na	95.42
33	magnetite		0.09	0.59	1.48	92.35	0.23	0.66	0.36	na	na	0.01	0.00	na	na	95.77
34	magnetite		0.07	0.64	1.47	91.07	0.28	0.73	0.47	na	na	0.01	0.04	na	na	94.77
35	magnetite		0.06	0.11	0.82	92.38	0.29	0.88	0.37	na	na	0.05	0.03	na	na	94.99

Table 7. Electron microprobe analyses (wt%) of silicate crystals in a thin section of a slag from site SPK4 at Kgopolwe Hill. Clinopyroxenes (cpx) are recalculated as percentages of hypothetical endmembers $Ca_2Si_2O_6$ (wollastonite), $Mg_2Si_2O_6$ (enstatite) and $Fe_2Si_2O_6$ (ferrosilite), and the averages of these values are plotted on Fig. 9.

Analysis	Mineral		SiO_2	TiO_2	Al_2O_3	FeO	MnO	MgO	CaO	K_2O	Na_2O	Cr_2O_3	CuO	P_2O_5	Total	$Ca_2Si_2O_6$	Mg_2SiO_6	$Fe_2Si_2O_6$
1	phosphate		0.06	0.00	0.01	0.03	0.02	0.00	55.22	0.00	0.05	0.00	0.00	40.62	96.01			
2	cpx		52.84	0.23	0.29	5.67	0.09	16.35	23.64	0.00	0.00	0.01	0.08	0.04	99.22	46.52	44.77	8.71
3	cpx		52.92	0.23	0.29	5.65	0.10	16.32	23.53	0.00	0.03	0.01	0.00	0.04	99.13	46.46	44.83	8.71
4	cpx		51.62	0.27	0.56	5.87	0.10	16.3	23.52	0.00	0.06	0.02	0.01	0.77	99.10	46.32	44.46	9.02
5	cpx		53.23	0.17	0.22	5.31	0.09	16.57	23.78	0.00	0.04	0.01	0.00	0.02	99.45	46.65	45.22	8.13
6	cpx		53.02	0.17	0.22	5.22	0.11	16.65	23.58	0.00	0.03	0.02	0.00	0.01	99.04	46.25	45.44	8.31
7	cpx		53.33	0.20	0.31	5.43	0.09	16.32	23.82	0.00	0.03	0.01	0.00	0.01	99.54	46.92	44.73	8.35
8	cpx		53.04	0.23	0.27	5.38	0.10	16.71	23.62	0.00	0.04	0.01	0.03	0.06	99.48	46.25	45.53	8.22
9	cpx		52.07	0.24	0.42	5.43	0.08	16.64	23.3	0.00	0.06	0.01	0.00	0.59	98.87	45.96	45.67	8.36
10	cpx		53.14	0.30	0.37	6.62	0.10	15.44	23.44	0.02	0.06	0.00	0.14	0.04	99.66	46.8	42.89	10.32
11	cpx		52.35	0.27	0.51	5.63	0.08	16.53	23.32	0.01	0.08	0.00	0.00	0.59	99.36	45.98	45.35	8.67
12	cpx		52.90	0.29	0.35	6.18	0.10	16.78	22.54	0.01	0.05	0.00	0.02	0.16	99.36	44.45	46.04	9.51
13	olivine	core	36.91	0.03	0.00	21.61	0.25	38.35	1.15	0.00	0.04	0.00	0.10	1.28	99.74			
14	olivine	core	36.96	0.04	0.00	23.68	0.25	37.20	1.16	0.00	0.04	0.00	0.05	0.68	100.05			
15	olivine	core	36.89	0.03	0.00	21.80	0.23	38.40	1.19	0.00	0.04	0.00	0.08	1.57	100.24			
16	olivine	rim	33.23	0.10	0.01	44.04	0.66	18.95	2.63	0.03	0.06	0.04	0.16	0.11	100.03			
17	olivine	core	35.50	0.07	0.00	29.91	0.39	31.53	1.13	0.00	0.02	0.03	0.06	1.10	99.75			
18	olivine	core	33.62	0.09	0.01	40.12	0.66	23.33	1.62	0.01	0.05	0.04	0.14	0.83	100.52			
19	olivine	rim	30.78	0.17	0.07	52.07	0.96	11.54	2.55	0.03	0.08	0.06	0.25	0.99	99.55			
20	olivine	core	35.64	0.06	0.00	28.50	0.36	32.61	1.22	0.01	0.05	0.02	0.03	1.27	99.78			
21	olivine	core	35.67	0.04	0.00	28.03	0.36	33.39	1.20	0.02	0.02	0.02	0.03	1.27	100.05			
22	olivine	rim	31.42	0.07	0.03	50.9	0.86	12.79	2.08	0.01	0.03	0.00	0.04	0.41	98.65			

Table 8. Electron microprobe analyses (wt%) of silicate crystals in a thin section of a slag from site SPM1 at Matsepe (Serotwe) Hill.

Analysis	Mineral	SiO_2	TiO_2	Al_2O_3	Cr_2O_3	FeO	MnO	MgO	CaO	Na_2O	K_2O	Total
1	melilite	42.54	0.00	0.96	0.00	7.73	0.08	9.27	38.35	0.31	0.12	99.34
2	monticellite	35.42	0.01	0.03	0.01	19.31	0.25	15.72	29.00	0.05	0.00	99.80
3	monticellite	36.05	0.01	0.00	0.03	16.64	0.19	17.75	29.12	0.04	0.00	99.83
4	monticellite	35.79	0.00	0.02	0.01	16.91	0.21	17.32	29.48	0.03	0.00	99.77
5	monticellite	35.69	0.00	0.01	0.02	17.21	0.26	17.55	28.87	0.04	0.01	99.65
6	monticellite	35.26	0.01	0.00	0.00	19.73	0.23	15.11	28.85	0.04	0.00	99.24
7	monticellite	35.78	0.02	0.02	0.00	18.32	0.24	16.83	28.65	0.04	0.00	99.90
8	monticellite	35.50	0.01	0.00	0.00	18.52	0.23	16.48	28.70	0.02	0.00	99.47
9	monticellite	32.19	0.01	0.01	0.00	36.58	0.32	5.00	24.33	0.09	0.01	98.53
10	monticellite	34.91	0.00	0.01	0.00	22.12	0.25	13.64	28.48	0.02	0.01	99.44
11	monticellite	32.54	0.01	0.01	0.00	33.27	0.38	5.65	26.55	0.08	0.02	98.51
12	monticellite	34.94	0.01	0.02	0.00	23.09	0.23	13.22	27.79	0.03	0.00	99.31
13	monticellite	35.06	0.02	0.01	0.00	20.92	0.25	14.68	28.91	0.04	0.00	99.89
14	monticellite	35.93	0.00	0.00	0.00	17.21	0.24	17.25	29.21	0.01	0.01	99.86
15	monticellite	33.95	0.00	0.01	0.00	26.74	0.29	10.52	27.62	0.03	0.00	99.15
16	monticellite	34.50	0.00	0.00	0.01	24.25	0.28	12.43	27.84	0.03	0.01	99.35

17	monticellite	35.26	0.00	0.01	0.01	20.32	0.26	15.08	28.73	0.07	0.01	99.74
18	monticellite	35.49	0.00	0.01	0.01	20.37	0.26	15.43	28.68	0.04	0.00	100.28
19	monticellite	34.78	0.00	0.02	0.00	23.00	0.23	13.20	28.18	0.05	0.00	99.46
20	monticellite	34.91	0.00	0.02	0.01	23.14	0.27	12.87	28.74	0.04	0.00	99.99
21	monticellite	35.12	0.00	0.02	0.00	19.41	0.24	15.51	28.96	0.09	0.03	99.37
22	monticellite	35.60	0.00	0.01	0.00	18.74	0.25	15.95	28.98	0.05	0.00	99.59
23	monticellite	35.55	0.00	0.01	0.00	20.27	0.29	15.10	28.63	0.04	0.01	99.91
24	monticellite	35.65	0.00	0.02	0.00	18.43	0.26	16.80	28.76	0.04	0.01	99.96
25	monticellite	35.12	0.01	0.01	0.01	20.37	0.26	15.24	28.48	0.04	0.00	99.53
26	monticellite	35.59	0.00	0.00	0.00	19.77	0.25	15.77	28.66	0.02	0.00	100.06
28	monticellite	35.31	0.00	0.02	0.00	19.45	0.25	15.80	28.58	0.04	0.01	99.45

Table 9. Electron microprobe analyses (wt%) and recalculation of hedenbergite crystals in a thin section of a slag from site SPM1 at Matsepe (Serotwe) Hill.

Microprobe analyses			
SiO_2	44.70	44.42	46.55
TiO_2	0.19	0.24	0.15
Al_2O_3	3.46	3.75	3.20
Cr_2O_3	0.00	0.01	0.02
FeO	19.71	19.82	17.99
MnO	0.08	0.09	0.11
MgO	7.30	6.90	8.00
CaO	22.91	23.00	23.33
Na_2O	0.08	0.08	0.09
Total	98.43	98.31	99.42
Recalculated as pyroxene with Fe3+			
SiO_2	44.70	44.42	46.55
TiO_2	0.19	0.24	0.15
Al_2O_3	3.46	3.75	3.20
Cr_2O_3	0.00	0.01	0.02
Fe_2O_3	9.89	9.70	7.62
FeO	10.81	11.09	11.13
MnO	0.08	0.09	0.11
MgO	7.30	6.90	8.00
CaO	22.91	23.00	23.33
Na_2O	0.08	0.08	0.09
Total	99.42	99.27	100.18
As fractions of hypothetical end-member pyroxenes			
$Ca_2Si_2O_6$	47.28	47.86	48.1
$Mg_2Si_2O_6$	20.96	19.96	22.95
$Fe_2Si_2O_6$	31.75	32.18	28.95

Table 10. SEM-EDS 'bulk' analysis of a copper slag, and averages of electron microprobe analyses of oxide and silicate phases from site GM10Mat Maranda. Low totals reflect the probable presence of ferric iron in all phases.

Phase	Method	no. Anls.	SiO_2	TiO_2	Al_2O_3	Cr_2O_3	FeO	MnO	MgO	CaO	K_2O	Na_2O	NiO	CuO	ZnO	P_2O_5	V_2O_5	SO_3	Total
'bulk'	SEM-EDS	5	44.90	0.40	5.40		42.70	0.10	0.50	3.00	0.50	0.40		0.60	1.20	0.20		0.10	100.00
spinel	Microprobe	3	0.71	1.49	3.28	0.07	83.35	0.03	0.18	0.13	0.06	0.01	0.05	0.07	1.78		0.19		91.40
fayalite	Microprobe	5	30.08	0.04	0.57	0.01	60.55	0.11	2.52	1.24	0.08	0.11	0.04	0.11	2.30		0.03		97.79
pyroxene 1	Microprobe	4	41.52	0.22	7.38	0.01	29.18	1.25	0.04	17.91	0.08	0.01	0.01	0.04	1.20		0.04		98.89
pyroxene 2	Microprobe	8	41.86	0.41	4.13	0.02	45.50	0.92	0.08	1.44	0.35	0.75	0.01	0.41	0.90		0.05		96.81
glass	Microprobe	5	53.84	1.27	11.01	0.02	19.77	0.14	0.05	8.55	0.57	1.27	0.01	0.26	0.34		0.07		97.17